

FCNC charmed-hadron decays with invisible singlet particles in light of recent data

Geng Li^{1a} and Jusak Tandean^{2b}

¹*School of Fundamental Physics and Mathematical Sciences,
Hangzhou Institute for Advanced Study,
UCAS, 310024 Hangzhou, China
University of Chinese Academy of Sciences,
100190 Beijing, China*

²*Tsung-Dao Lee Institute,
Shanghai Jiao Tong University,
Shanghai 201210, China*

Abstract

The flavor-changing neutral current (FCNC) decays of charmed hadrons with missing energy (\cancel{E}) can serve as potentially promising hunting grounds for hints of new physics, as the standard-model backgrounds are very suppressed. A few of such processes have been searched for in recent experiments, specifically $D^0 \rightarrow \cancel{E}$ by Belle and $D^0 \rightarrow \pi^0 \cancel{E}$ and $\Lambda_c^+ \rightarrow p \cancel{E}$ by BESIII, resulting in upper bounds on their branching fractions. We consider them to illuminate the possible contributions of the quark transition $c \rightarrow u \cancel{E}$ with a couple of invisible spinless bosons carrying away the missing energy, assuming that they are not charge conjugates of each other and hence can have unequal masses. We find that these data are complementary in that they constrain different sets of the underlying operators and do not cover the same ranges of the bosons' masses, but there are regions not yet accessible. From the allowed parameter space, we show that other D -meson decays, such as $D \rightarrow \rho \cancel{E}$, and the charmed-baryon ones $\Xi_c \rightarrow (\Sigma, \Lambda) \cancel{E}$ can have sizable branching fractions and therefore may offer further probes of the new-physics interactions. We point out the importance of $D^0 \rightarrow \gamma \cancel{E}$ which are not yet searched for but could access parts of the parameter space beyond the reach of the other modes. In addition, we look at a scenario where the invisibles are instead fermionic, namely sterile neutrinos, and a scalar leptoquark mediates $c \rightarrow u \cancel{E}$. We discuss the implications of the aforesaid bounds for this model. The predictions we make for the various charmed-hadron decays in the different scenarios may be testable in the near future by BESIII and Belle II.

^a ligeng@ucas.ac.cn

^b jtandean@yahoo.com

I. INTRODUCTION

Flavor-changing neutral current (FCNC) hadron decays that alter the charm quantum number by one unit ($|\Delta C| = 1$) and have missing energy (\cancel{E}) in the final states have received lots of theoretical attention over the years [1–26] because they are potentially valuable tools in the hunt for evidence of new physics (NP) beyond the standard model (SM). In the SM such processes receive both short- and long-distance contributions. The former comes from the quark transition $c \rightarrow uv\bar{\nu}$, with undetected neutrinos ($\nu\bar{\nu}$) being emitted, and is much suppressed because it arises from loop diagrams and is subject to highly efficient Glashow-Iliopoulos-Maiani cancellation. Explicitly, the updated predictions for the branching fractions of a number of charmed-hadron modes of interest due to the short-distance SM physics alone are

$$\begin{aligned}
 \mathcal{B}(D^0 \rightarrow \nu\bar{\nu})_{\text{SM}} &= 0, & \mathcal{B}(D^0 \rightarrow \gamma\nu\bar{\nu})_{\text{SM}} &= 1.8 \times 10^{-19}, \\
 \mathcal{B}(D^0 \rightarrow \pi^0\nu\bar{\nu})_{\text{SM}} &= 2.5 \times 10^{-17}, & \mathcal{B}(D^0 \rightarrow \rho^0\nu\bar{\nu})_{\text{SM}} &= 1.1 \times 10^{-17}, \\
 \mathcal{B}(D^+ \rightarrow \pi^+\nu\bar{\nu})_{\text{SM}} &= 1.3 \times 10^{-16}, & \mathcal{B}(D^+ \rightarrow \rho^+\nu\bar{\nu})_{\text{SM}} &= 5.9 \times 10^{-17}, \\
 \mathcal{B}(D_s^+ \rightarrow K^+\nu\bar{\nu})_{\text{SM}} &= 4.5 \times 10^{-17}, & \mathcal{B}(D_s^+ \rightarrow K^{*+}\nu\bar{\nu})_{\text{SM}} &= 3.3 \times 10^{-17}, \\
 \mathcal{B}(\Lambda_c^+ \rightarrow p\nu\bar{\nu})_{\text{SM}} &= 7.3 \times 10^{-17}, & \mathcal{B}(\Xi_c^+ \rightarrow \Sigma^+\nu\bar{\nu})_{\text{SM}} &= 1.1 \times 10^{-16}, \\
 \mathcal{B}(\Xi_c^0 \rightarrow \Sigma^0\nu\bar{\nu})_{\text{SM}} &= 1.8 \times 10^{-17}, & \mathcal{B}(\Xi_c^0 \rightarrow \Lambda\nu\bar{\nu})_{\text{SM}} &= 6.5 \times 10^{-18},
 \end{aligned} \tag{1}$$

as evaluated later on in an appendix. The long-distance components have been estimated to be minuscule as well [2, 5, 14].

In the presence of NP, the SM amplitudes might be modified and/or there might be extra channels involving one or more invisible nonstandard particles. These are factors that could substantially enhance the rates. Since the SM backgrounds are minimal, an observation of any of these decays at the present or near-future sensitivity level would likely be a sign of NP.

To date, there have been only a handful of attempts to seek FCNC $|\Delta C| = 1$ transitions with missing energy, which came up empty, and the null outcomes translated into upper limits on their branching fractions [27–30]. The parent hadrons examined in these measurements, performed by the Belle and BESIII Collaborations, were the neutral pseudoscalar charmed-meson D^0 and the singly-charmed spin-1/2 baryon Λ_c^+ . Belle announced $\mathcal{B}(D^0 \rightarrow \text{invisibles}) < 9.4 \times 10^{-5}$ [28], while BESIII reported $\mathcal{B}(D^0 \rightarrow \pi^0\nu\bar{\nu}) < 2.1 \times 10^{-4}$ [29] and $\mathcal{B}(\Lambda_c^+ \rightarrow p\gamma')$ $< 8.0 \times 10^{-5}$ [30], all at 90% confidence level, with γ' denoting a massless dark photon, which was unobservable. In light of the smallness of the SM predictions above and the lack or scarcity of the corresponding experimental information, it is clear that the window of opportunity to discover NP in any one of these modes is wide open.

In view of their significance as beneficial probes of NP, it is hoped that more and more quests will be carried out for these kind of processes at already running operations, especially BESIII and Belle II. At least it is anticipated that BESIII could better its aforementioned $D^0 \rightarrow \pi^0\nu\bar{\nu}$ result [29] by a factor of ~ 3 after its data sample gathered at center-of-mass energy $\sqrt{s} \simeq 3.77 \text{ GeV}$

is increased from 2.93 fb^{-1} to 20 fb^{-1} in a few years [29, 31]. In addition, Belle II is expected to improve on the Belle bound on $D^0 \rightarrow$ invisibles by a factor of seven [32], and BESIII might push it down further to 10^{-6} with its final charm dataset [31]. The foregoing suggests that for $D^0 \rightarrow \pi^0 \nu \bar{\nu}$ the ultimate reach of Belle II might be less than that of BESIII. More distant in the future, searches for these decays with greater levels of sensitivity would presumably be feasible at the proposed Super Tau-Charm Facility (STCF), Circular Electron Positron Collider (CEPC), and Future Circular e^+e^- Collider (FCC-ee). The STCF [33] is designed to accumulate a data sample about 100 times that collected by BESIII and could therefore improve on the latter’s reach for the preceding D^0 modes by a factor of 10 or better. At the CEPC and FCC-ee, operating as Z -boson factories, the projected numbers of D^0 (and its antiparticle) from $Z \rightarrow c\bar{c}$ are 1×10^{11} [34] and 6×10^{11} [13, 35], respectively. Since Belle II is anticipated to yield 8×10^{10} of these mesons [13], the CEPC and FCC-ee would expectedly be somewhat superior to Belle II for probing $D^0 \rightarrow \cancel{E}, \pi^0 \cancel{E}$ if the three have similar reconstruction efficiencies. Given that the D^0 amount collected in each of these ongoing and proposed experiments [13, 31, 32, 34] is bigger than those of the $D_{(s)}^+$ meson and charmed baryons, the sensitivities of these facilities to the other FCNC charmed-hadron transitions we will look at would probably be comparable or lower.

The prospect that a growing amount of fresh data on this subject is forthcoming has lately revived related theoretical efforts [7–26]. Various aspects of it have been explored to different extents, including the type of particles carrying away the missing energy and how many of them. They might be a pair of ordinary neutrinos, and this often means that the restraints on the interactions of their charged-lepton partners would at the same time squeeze the room for the NP affecting the dineutrino decays [10–17]. Alternatively, the invisibles could be spin-1/2 fermions [6–10] or a pair of spin-0 bosons [6, 20, 22] which hail from beyond the SM and are singlets under the SM gauge groups, implying that the restrictions pertaining to the charged leptons would likely have little, if any, bearing on the $c \rightarrow u \cancel{E}$ sector. Another possibility is that the missing energy is carried away instead by just one particle which is again a SM-gauge singlet and has to be a boson. It might be spinless [19–21] or has spin 1, such as the massless dark photon [23–25]. It is worth remarking that similar transitions among down-type quarks with invisible bosons have also been much discussed in the past [6, 20–24, 36–51]¹ and the bosons might be dark-matter candidates.

Here we adopt a model-independent approach to investigate the decays of charmed hadrons brought about by effective $c \rightarrow u \cancel{E}$ operators in which the invisibles comprise a couple of SM-gauge-singlet spin-0 bosons.² Unlike in most earlier papers, we assume that these particles are not charge conjugates of one another and hence may not have the same mass. It turns out that whether or not their masses are equal could determine the feasibility of probing their couplings

¹ Corresponding processes with invisible new fermions have recently been analyzed in, *e.g.*, refs. [49–55].

² The two bosons could alternatively be of spin 1. As can be inferred from refs. [6, 40, 47], the situation would then be significantly more complicated than its spin-0 counterpart, with a much bigger number of effective operators, and, on top of that, their coefficients would have relatively far weaker experimental bounds [40, 47]. For these reasons, we opt not to deal with the spin-1 case here.

to the quarks. Furthermore, taking into account the Belle and BESIII data quoted above and anticipating related upcoming measurements, we address a number of charmed-hadron processes, not only $D^0 \rightarrow \cancel{E}, \pi^0 \cancel{E}$ and $\Lambda_c^+ \rightarrow p \cancel{E}$ but also $D^0 \rightarrow \gamma \cancel{E}$, more decays of pseudoscalar charmed-mesons into final states with a charmless meson, and analogous decays of the singly-charmed baryons Ξ_c^+ and Ξ_c^0 . After extracting the allowed couplings from the existing empirical constraints, we make predictions for these proposed modes which are potentially testable soon. Moreover, we demonstrate that $D^0 \rightarrow \gamma \cancel{E}$ besides $D^0 \rightarrow \cancel{E}$ would be especially advantageous, as it could access parameter space that is outside the reach of the other decays.

We also examine the case where singlet spin-1/2 fermions instead act as the invisibles. We suppose in particular that they are connected to the u and c quarks owing to their joint couplings to a scalar leptoquark. This was first treated in detail in ref. [10], where the singlet fermions' masses were taken to be negligible and consequently the already available limit on $D^0 \rightarrow \cancel{E}$ from Belle did not apply. The advent of the BESIII limits on $D^0 \rightarrow \pi^0 \cancel{E}$ and $\Lambda_c^+ \rightarrow p \cancel{E}$ has opened up an opportunity to scrutinize the model more thoroughly, and with the invisible fermions' masses permitted to be nonzero the Belle result becomes relevant as well. Thus, as in the bosonic scenario, we will explore the implications of these recent data for several analogous FCNC charmed-hadron decays with missing energy. From all this exercise, we hope to learn some of the salient consequences of selecting different types of invisible particles and of doing a model-based study versus a model-independent one.

The structure of the remainder of the paper is the following. In the next section, we first write down the operators for the effective $c \rightarrow u \cancel{E}$ transition with the invisible light spinless bosons and subsequently derive the induced amplitudes for the hadron decays investigated here and the corresponding rates. With them we perform the numerical analysis in section III. In section IV we entertain the possibility that the invisibles produced in $c \rightarrow u \cancel{E}$ are singlet spin-1/2 fermions. In section V we give our conclusions. In two appendices we specify the hadronic form factors needed in our computation and estimate the SM backgrounds to the various modes with missing energy.

II. INTERACTIONS AND HADRON DECAYS DUE TO $c \rightarrow u \cancel{S}'$

The invisible light spin-0 bosons are SM-gauge singlets described by complex fields \mathbf{S} and \mathbf{S}' . They could be stable or sufficiently long-lived to escape detection. We assume that they are charged under some dark-sector symmetry or odd under a Z_2 symmetry, $\mathbf{S}^{(\prime)} \rightarrow -\mathbf{S}^{(\prime)}$, which does not influence SM fields. Accordingly, \mathbf{S} and \mathbf{S}' do not interact singly with SM quarks. The leading-order low-energy effective $|\Delta C|=1$ operators containing these bosons are expressible as [6, 40]

$$\mathcal{L}_{\mathbf{S}\mathbf{S}'} = -(\kappa_{\mathbf{S}\mathbf{S}'}^{\mathbf{V}} \bar{u} \gamma_\mu c + \kappa_{\mathbf{S}\mathbf{S}'}^{\mathbf{A}} \bar{u} \gamma_\mu \gamma_5 c) i(\mathbf{S}^\dagger \partial^\mu \mathbf{S}' - \partial^\mu \mathbf{S}^\dagger \mathbf{S}') - (\kappa_{\mathbf{S}\mathbf{S}'}^{\mathbf{S}} \bar{u} c + \kappa_{\mathbf{S}\mathbf{S}'}^{\mathbf{P}} \bar{u} \gamma_5 c) m_c \mathbf{S}^\dagger \mathbf{S}' + \text{H.c.}, \quad (2)$$

where $\kappa_{\mathbf{S}\mathbf{S}'}^{\mathbf{X}}$, $\mathbf{X} = \mathbf{V}, \mathbf{A}, \mathbf{S}, \mathbf{P}$, are in general complex coefficients which have the dimensions of inverse squared mass and m_c is the charm-quark mass. These κ s are free parameters in our model-independent approach and will be treated phenomenologically in our numerical work. We notice in

$\mathcal{L}_{SS'}$ that $\kappa_{SS'}^V$ and $\kappa_{SS'}^S$ ($\kappa_{SS'}^A$ and $\kappa_{SS'}^P$) accompany quark bilinears which are parity even (odd). We suppose that $S' \neq S$ and hence their masses can be unequal.³

It is interesting to comment that the emitted bosons not being charged conjugates of each other is beneficial because that helps avoid extra restrictions from the data on D^0 - \bar{D}^0 mixing. For the latter gets contributions from four-quark operators $\bar{u}(1, \gamma^\alpha)\gamma_5 c \bar{u}(1, \gamma_\alpha)\gamma_5 c$ that are generated by loop diagrams with S and S' being in the loops and have coefficients proportional to linear combinations of $\kappa_{SS'}^X \kappa_{S'S}^X$, with $X = V, A, S, P$, which vanish if $S' \neq S$ and $\kappa_{S'S}^X = 0$.⁴ The operators in $\mathcal{L}_{SS'}$ give rise to many sorts of FCNC decays of charmed hadrons with missing energy. Here we focus on the processes represented by the diagrams collected in figure 1. As already stated, the corresponding transitions in the SM, which have neutrinos in the final states, are highly suppressed. Based on prior calculations [1, 2, 6, 19] and the updated estimates in appendix B, we can safely ignore the SM backgrounds to these hadron modes. In the rest of this section, we discuss in detail the amplitudes for the latter and their rates.

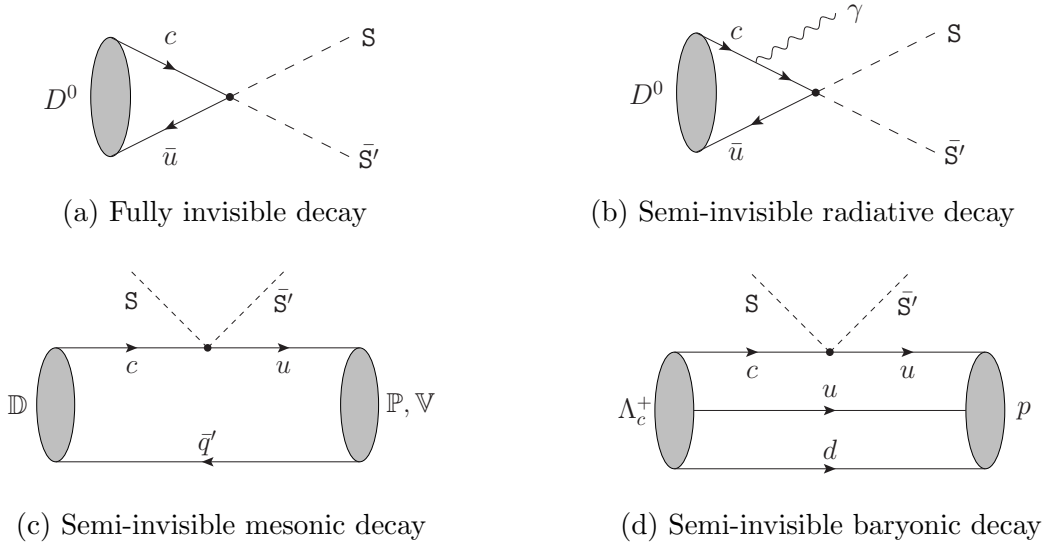


FIG. 1. Diagrams of FCNC charmed-hadron decays with two invisible light spin-0 bosons. In (b) the photon can also be emitted from the \bar{u} -quark line.

A. Fully invisible decay

The amplitude for the invisible channel $D^0 \rightarrow S\bar{S}'$ can be expressed as

$$\mathcal{M}_{D^0 \rightarrow S\bar{S}'} = \kappa_{SS'}^A \langle 0 | \bar{u} \gamma^\mu \gamma_5 c | D^0 \rangle (\mathbf{k} - \mathbf{k}')_\mu + \kappa_{SS'}^P m_c \langle 0 | \bar{u} \gamma_5 c | D^0 \rangle, \quad (3)$$

³ Effective operators for quark FCNCs involving two invisible light new particles which may differ in mass have been considered before in the literature, such as refs. [48, 50] ([10, 49, 50]) where the invisibles are dark spin-0 bosons (spin-1/2 fermions).

⁴ Similar situations occur in section IV and in the strangeness-changing (kaon and hyperon) sector [49, 53].

with the mesonic matrix elements

$$\langle 0|\bar{u}\gamma^\mu\gamma_5c|D^0\rangle = -if_D p_{D^0}^\mu, \quad \langle 0|\bar{u}\gamma_5c|D^0\rangle = \frac{if_D m_{D^0}^2}{m_u + m_c}, \quad (4)$$

where f_D stands for the D^0 decay constant and p_X (m_X) is the momentum (mass) of X . There are no contributions of $\kappa_{\mathbf{S}\mathbf{S}'}^{\mathbf{S}}$ and $\kappa_{\mathbf{S}\mathbf{S}'}^{\mathbf{V}}$ because $\langle 0|\bar{u}\gamma^\mu c|D^0\rangle = \langle 0|\bar{u}c|D^0\rangle = 0$. Neglecting m_u compared to m_c then leads to

$$\mathcal{M}_{D^0 \rightarrow \mathbf{S}\bar{\mathbf{S}}'} = i[\kappa_{\mathbf{S}\mathbf{S}'}^{\mathbf{A}}(m_{\mathbf{S}'}^2 - m_{\mathbf{S}}^2) + \kappa_{\mathbf{S}\mathbf{S}'}^{\mathbf{P}}m_{D^0}^2]f_D. \quad (5)$$

From this follows the rate

$$\Gamma_{D^0 \rightarrow \mathbf{S}\bar{\mathbf{S}}'} = \frac{\lambda^{1/2}(m_{D^0}^2, m_{\mathbf{S}}^2, m_{\mathbf{S}'}^2)}{16\pi m_{D^0}^3} |\kappa_{\mathbf{S}\mathbf{S}'}^{\mathbf{A}}(m_{\mathbf{S}'}^2 - m_{\mathbf{S}}^2) + \kappa_{\mathbf{S}\mathbf{S}'}^{\mathbf{P}}m_{D^0}^2|^2 f_D^2, \quad (6)$$

which contains the Källén function $\lambda(x, y, z) = x^2 + y^2 + z^2 - 2(xy + xz + yz)$. Evidently, $D^0 \rightarrow \mathbf{S}\bar{\mathbf{S}}'$ can in general probe $\kappa_{\mathbf{S}\mathbf{S}'}^{\mathbf{P}}$ and $\kappa_{\mathbf{S}\mathbf{S}'}^{\mathbf{A}}$, which accompany the parity-odd quark bilinears in $\mathcal{L}_{\mathbf{S}\mathbf{S}'}$, but the sensitivity to $\kappa_{\mathbf{S}\mathbf{S}'}^{\mathbf{A}}$ will be lost if $m_{\mathbf{S}'} = m_{\mathbf{S}}$.

B. Semi-invisible radiative decay

Although $\kappa_{\mathbf{S}\mathbf{S}'}^{\mathbf{V}}$ has no impact on the preceding mode, as does $\kappa_{\mathbf{S}\mathbf{S}'}^{\mathbf{A}}$ if \mathbf{S} and \mathbf{S}' are degenerate, these parameters can contribute together if an ordinary photon is radiated, namely in $D^0 \rightarrow \gamma\mathbf{S}\bar{\mathbf{S}}'$. The amplitude for it is

$$\mathcal{M}_{D^0 \rightarrow \gamma\mathbf{S}\bar{\mathbf{S}}'} = \kappa_{\mathbf{S}\mathbf{S}'}^{\mathbf{V}} \langle \gamma|\bar{u}\gamma_\mu c|D^0\rangle (\mathbf{k} - \mathbf{k}')^\mu + \kappa_{\mathbf{S}\mathbf{S}'}^{\mathbf{A}} \langle \gamma|\bar{u}\gamma^\mu\gamma_5c|D^0\rangle (\mathbf{k} - \mathbf{k}')_\mu, \quad (7)$$

where $\mathbf{k}^{(n)}$ designates the momentum of $\mathbf{S}^{(n)}$ and

$$\langle \gamma|\bar{u}\gamma_\mu c|D^0\rangle = \frac{eF_V}{m_{D^0}} \epsilon_{\mu\zeta\eta\theta} \varepsilon_\gamma^{\zeta*} p_{D^0}^\eta p_\gamma^\theta, \quad \langle \gamma|\bar{u}\gamma^\mu\gamma_5c|D^0\rangle = \frac{ieF_A}{m_{D^0}} (p_\gamma \cdot p_{D^0} \varepsilon_\gamma^{\mu*} - \varepsilon_\gamma^* \cdot p_{D^0} p_\gamma^\mu), \quad (8)$$

with e being the proton charge, ε_X denoting the polarization vector of X , and F_V and F_A symbolizing form factors depending on the squared momentum-transfer $(p_{D^0} - p_\gamma)^2 = (\mathbf{k} + \mathbf{k}')^2 \equiv \hat{s}$. Since $\langle \gamma|\bar{u}c|D^0\rangle = \langle \gamma|\bar{u}\gamma_5c|D^0\rangle = 0$, there are no $\kappa_{\mathbf{S}\mathbf{S}'}^{\mathbf{S},\mathbf{P}}$ terms in eq. (7). It is obvious that $\mathcal{M}_{D^0 \rightarrow \gamma\mathbf{S}\bar{\mathbf{S}}'}$ satisfies the requirement of electromagnetic gauge-invariance. Evaluating the absolute square of the amplitude times the three-body phase space, one obtains the differential rate

$$\frac{d\Gamma_{D^0 \rightarrow \gamma\mathbf{S}\bar{\mathbf{S}}'}}{d\hat{s}} = \frac{\alpha_e \lambda^{3/2}(\hat{s}, m_{\mathbf{S}}^2, m_{\mathbf{S}'}^2)}{384\pi^2 m_{D^0}^5 \hat{s}^2} (m_{D^0}^2 - \hat{s})^3 (|\kappa_{\mathbf{S}\mathbf{S}'}^{\mathbf{V}}|^2 F_V^2 + |\kappa_{\mathbf{S}\mathbf{S}'}^{\mathbf{A}}|^2 F_A^2), \quad (9)$$

which is to be integrated over $(m_{\mathbf{S}} + m_{\mathbf{S}'}^2)^2 \leq \hat{s} \leq m_{D^0}^2$. Thus, the invisible scalars' mass range covered by this mode is $0 \leq m_{\mathbf{S}} + m_{\mathbf{S}'} < m_{D^0}$, the same as that in the $D^0 \rightarrow \mathbf{S}\bar{\mathbf{S}}'$ case. All this illustrates the importance of $D^0 \rightarrow \gamma\cancel{\mathbf{S}}\bar{\mathbf{S}}'$ as a valuable search tool for new physics, despite its rate having a suppression factor of $\alpha_e = e^2/(4\pi) = 1/137$.

C. Semi-invisible mesonic decays

The interactions in $\mathcal{L}_{\text{SS}'}$ can cause a pseudoscalar charmed-meson \mathbb{D} to turn into a pseudoscalar or vector charmless-meson, \mathbb{P} or \mathbb{V} , plus the $\text{S}\bar{\text{S}}'$ pair. Specifically, we will look at the instances where $\mathbb{D} = D^0, D^+, D_s^+$ and the final mesons are $\mathbb{P} = \pi^0, \pi^+, K^+$ or $\mathbb{V} = \rho^0, \rho^+, K^{*+}$, respectively. The amplitudes for these channels are

$$\mathcal{M}_{\mathbb{D} \rightarrow \text{P}\bar{\text{S}}\text{S}'} = \kappa_{\text{SS}'}^{\text{V}} \langle \text{P} | \bar{u} \gamma^\mu c | \mathbb{D} \rangle (\mathbf{k} - \mathbf{k}')_\mu + \kappa_{\text{SS}'}^{\text{S}} m_c \langle \text{P} | \bar{u} c | \mathbb{D} \rangle, \quad (10)$$

$$\mathcal{M}_{\mathbb{D} \rightarrow \text{V}\bar{\text{S}}\text{S}'} = \kappa_{\text{SS}'}^{\text{V}} \langle \text{V} | \bar{u} \gamma_\mu c | \mathbb{D} \rangle (\mathbf{k} - \mathbf{k}')^\mu + \kappa_{\text{SS}'}^{\text{A}} \langle \text{V} | \bar{u} \gamma^\mu \gamma_5 c | \mathbb{D} \rangle (\mathbf{k} - \mathbf{k}')_\mu + \kappa_{\text{SS}'}^{\text{P}} m_c \langle \text{V} | \bar{u} \gamma_5 c | \mathbb{D} \rangle, \quad (11)$$

which involve the momentum $\mathbf{k}^{(\prime)}$ of $\text{S}^{(\prime)}$ and the mesonic matrix elements

$$\begin{aligned} \langle \text{P} | \bar{u} \gamma^\mu c | \mathbb{D} \rangle &= (p_{\mathbb{D}}^\mu + p_{\text{P}}^\mu) f_+ + (p_{\mathbb{D}}^\mu - p_{\text{P}}^\mu) (f_0 - f_+) \frac{m_{\mathbb{D}}^2 - m_{\text{P}}^2}{q_{\mathbb{D}\text{P}}^2}, \\ \langle \text{P} | \bar{u} c | \mathbb{D} \rangle &= \frac{m_{\mathbb{D}}^2 - m_{\text{P}}^2}{m_c - m_u} f_0, \\ \langle \text{V} | \bar{u} \gamma_\mu c | \mathbb{D} \rangle &= \frac{2V}{m_{\mathbb{D}} + m_{\text{V}}} \epsilon_{\mu\beta\eta\theta} \varepsilon_{\text{V}}^{\beta*} p_{\text{V}}^\eta p_{\mathbb{D}}^\theta, \\ \langle \text{V} | \bar{u} \gamma^\mu \gamma_5 c | \mathbb{D} \rangle &= i(m_{\mathbb{D}} + m_{\text{V}}) \varepsilon_{\text{V}}^{\mu*} A_1 - \left[\frac{p_{\mathbb{D}}^\mu + p_{\text{V}}^\mu}{m_{\mathbb{D}} + m_{\text{V}}} A_2 + \frac{p_{\mathbb{D}}^\mu - p_{\text{V}}^\mu}{q_{\mathbb{D}\text{V}}^2} (A_3 - A_0) 2m_{\text{V}} \right] i \varepsilon_{\text{V}}^* \cdot p_{\mathbb{D}}, \\ \langle \text{V} | \bar{u} \gamma_5 c | \mathbb{D} \rangle &= \frac{-2i A_0 m_{\text{V}}}{m_c + m_u} \varepsilon_{\text{V}}^* \cdot p_{\mathbb{D}}, \end{aligned} \quad (12)$$

where f_+ and f_0 [V, A_0, A_1 , and A_2] are form factors which are functions of the squared momentum-transfer $q_{\mathbb{D}\text{P}}^2 = (p_{\mathbb{D}} - p_{\text{P}})^2$ [$q_{\mathbb{D}\text{V}}^2 = (p_{\mathbb{D}} - p_{\text{V}})^2$] and $2A_3 m_{\text{V}} = (m_{\mathbb{D}} + m_{\text{V}}) A_1 - (m_{\mathbb{D}} - m_{\text{V}}) A_2$. Other $\kappa_{\text{SS}'}$ terms are absent from eqs. (10)-(11) because $\langle \text{P} | \bar{u} \gamma^\mu \gamma_5 c | \mathbb{D} \rangle = \langle \text{P} | \bar{u} \gamma_5 c | \mathbb{D} \rangle = \langle \text{V} | \bar{u} c | \mathbb{D} \rangle = 0$.

Given that $m_u = 0.002 m_c$, henceforth we ignore m_u relative to m_c when calculating decay rates. Accordingly, from the absolute squares of the amplitudes in eqs. (10)-(11), we arrive at

$$\begin{aligned} \frac{d\Gamma_{\mathbb{D} \rightarrow \text{P}\bar{\text{S}}\text{S}'}}{d\hat{s}} &= \frac{2\tilde{\lambda}_{\mathbb{D}\text{P}}^{1/2} \tilde{\lambda}_{\text{SS}'}^{1/2}}{(8\pi m_{\mathbb{D}} \hat{s})^3} \left[\frac{1}{3} |\kappa_{\text{SS}'}^{\text{V}}|^2 \tilde{\lambda}_{\mathbb{D}\text{P}} \tilde{\lambda}_{\text{SS}'} f_+^2 + |\kappa_{\text{SS}'}^{\text{S}} (m_{\text{S}}^2 - m_{\text{S}'}^2) + \kappa_{\text{SS}'}^{\text{S}} \hat{s}|^2 (m_{\mathbb{D}}^2 - m_{\text{P}}^2)^2 f_0^2 \right], \\ \frac{d\Gamma_{\mathbb{D} \rightarrow \text{V}\bar{\text{S}}\text{S}'}}{d\hat{s}} &= \frac{\tilde{\lambda}_{\mathbb{D}\text{V}}^{3/2} \tilde{\lambda}_{\text{SS}'}^{3/2}}{(8\pi m_{\mathbb{D}} \hat{s})^3} \left\{ \frac{|\kappa_{\text{SS}'}^{\text{A}}|^2}{6 m_{\text{V}}^2} \left[\left(1 + \frac{12 m_{\text{V}}^2 \hat{s}}{\tilde{\lambda}_{\mathbb{D}\text{V}}} \right) A_1^2 \tilde{m}_+^2 + 2(\hat{s} - \tilde{m}_+ \tilde{m}_-) A_1 A_2 + \frac{\tilde{\lambda}_{\mathbb{D}\text{V}} A_2^2}{\tilde{m}_+^2} \right] \right. \\ &\quad \left. + \frac{2A_0^2}{\tilde{\lambda}_{\text{SS}'}} |\kappa_{\text{SS}'}^{\text{A}} (m_{\text{S}'}^2 - m_{\text{S}}^2) + \kappa_{\text{SS}'}^{\text{P}} \hat{s}|^2 + \frac{4|\kappa_{\text{SS}'}^{\text{V}}|^2 \hat{s} V^2}{3 \tilde{m}_+^2} \right\}, \end{aligned} \quad (14)$$

to be integrated over $(m_{\text{S}} + m_{\text{S}'})^2 \leq \hat{s} = (\mathbf{k} + \mathbf{k}')^2 \leq (m_{\mathbb{D}} - m_{\text{P},\text{V}})^2$, respectively, with

$$\tilde{\lambda}_{\text{XY}} = \lambda(m_{\text{X}}^2, m_{\text{Y}}^2, \hat{s}), \quad \tilde{m}_{\pm} = m_{\mathbb{D}} \pm m_{\text{V}}. \quad (15)$$

In eq. (14), we see that $\mathbb{D} \rightarrow \text{P}\bar{\text{S}}\text{S}'$ can probe not only $\kappa_{\text{SS}'}^{\text{V}}$, but also $\kappa_{\text{SS}'}^{\text{S}}$, which is inaccessible to $D^0 \rightarrow \text{S}\bar{\text{S}}', \gamma\text{S}\bar{\text{S}}'$ as well as to $\mathbb{D} \rightarrow \text{V}\bar{\text{S}}\text{S}'$. However, the latter is sensitive to the other three parameters, $\kappa_{\text{SS}'}^{\text{V,P,A}}$.

D. Semi-invisible baryonic decays

Given that at the moment the empirical information on FCNC $|\Delta C|=1$ decays with missing energy is still scarce, it is essential to investigate, in addition, this type of transitions among baryons. As we demonstrate shortly, they can play a complementary role in the quest for hints of new physics in $c \rightarrow u \cancel{E}$.

Of interest here are $\Lambda_c^+ \rightarrow p\mathbb{S}\bar{\mathbb{S}}'$ and $\Xi_c^{+,0} \rightarrow \Sigma^{+,0}\mathbb{S}\bar{\mathbb{S}}'$ plus $\Xi_c^0 \rightarrow \Lambda\mathbb{S}\bar{\mathbb{S}}'$, but we explicitly treat only the amplitude for the first decay and its rate, as the corresponding quantities for the other three have analogous formulas. Thus, we write

$$\begin{aligned} \mathcal{M}_{\Lambda_c^+ \rightarrow p\mathbb{S}\bar{\mathbb{S}}'} &= \kappa_{\mathbb{S}\bar{\mathbb{S}}'}^{\mathbb{V}} \langle p|\bar{u}\gamma^\mu c|\Lambda_c^+\rangle (\mathbf{k} - \mathbf{k}')_\mu + \kappa_{\mathbb{S}\bar{\mathbb{S}}'}^{\mathbb{A}} \langle p|\bar{u}\gamma^\mu \gamma_5 c|\Lambda_c^+\rangle (\mathbf{k} - \mathbf{k}')_\mu \\ &+ \kappa_{\mathbb{S}\bar{\mathbb{S}}'}^{\mathbb{S}} m_c \langle p|\bar{u}c|\Lambda_c^+\rangle + \kappa_{\mathbb{S}\bar{\mathbb{S}}'}^{\mathbb{P}} m_c \langle p|\bar{u}\gamma_5 c|\Lambda_c^+\rangle, \end{aligned} \quad (16)$$

where $\mathbf{k}^{(\prime)}$ is again the momentum of $\mathbb{S}^{(\prime)}$ and the baryonic matrix elements are expressible as

$$\begin{aligned} \langle p|\bar{u}\gamma^\mu c|\Lambda_c^+\rangle &= \bar{u}_p \left\{ \left[\gamma^\mu - \frac{\mathbf{M}_+ \hat{p}^\mu - \mathbf{M}_- \hat{q}^\mu}{\mathbf{M}_+^2 - \hat{q}^2} \right] \mathbf{F}_\perp + \left[\hat{p}^\mu - \frac{\mathbf{M}_+ \mathbf{M}_- \hat{q}^\mu}{\hat{q}^2} \right] \frac{\mathbf{M}_+ \mathbf{F}_+}{\mathbf{M}_+^2 - \hat{q}^2} + \frac{\mathbf{M}_- \hat{q}^\mu}{\hat{q}^2} \mathbf{F}_0 \right\} u_{\Lambda_c}, \\ \langle p|\bar{u}\gamma^\mu \gamma_5 c|\Lambda_c^+\rangle &= \bar{u}_p \left\{ \left[\gamma^\mu + \frac{\mathbf{M}_- \hat{p}^\mu - \mathbf{M}_+ \hat{q}^\mu}{\mathbf{M}_-^2 - \hat{q}^2} \right] \mathbf{G}_\perp - \left[\hat{p}^\mu - \frac{\mathbf{M}_+ \mathbf{M}_- \hat{q}^\mu}{\hat{q}^2} \right] \frac{\mathbf{M}_- \mathbf{G}_+}{\mathbf{M}_-^2 - \hat{q}^2} - \frac{\mathbf{M}_+ \hat{q}^\mu}{\hat{q}^2} \mathbf{G}_0 \right\} \gamma_5 u_{\Lambda_c}, \\ \langle p|\bar{u}c|\Lambda_c^+\rangle &= \frac{\mathbf{M}_- \mathbf{F}_0}{m_c - m_u} \bar{u}_p u_{\Lambda_c}, \quad \langle p|\bar{u}\gamma_5 c|\Lambda_c^+\rangle = \frac{\mathbf{M}_+ \mathbf{G}_0}{m_c + m_u} \bar{u}_p \gamma_5 u_{\Lambda_c}, \end{aligned} \quad (17)$$

where u_p and u_{Λ_c} designate the Dirac spinors of the baryons, $\mathbf{F}_{\perp,+0}$ and $\mathbf{G}_{\perp,+0}$ symbolize form factors which depend on $\hat{s} = \hat{q}^2$,

$$\mathbf{M}_\pm = m_{\Lambda_c} \pm m_p, \quad \hat{p} = p_{\Lambda_c} + p_p, \quad \hat{q} = p_{\Lambda_c} - p_p. \quad (18)$$

After averaging (summing) the absolute square of the amplitude over the initial (final) baryon polarizations and multiplying by the three-body phase space, we find the differential rate

$$\begin{aligned} \frac{d\Gamma_{\Lambda_c^+ \rightarrow p\mathbb{S}\bar{\mathbb{S}}'}}{d\hat{s}} &= \frac{2\tilde{\lambda}_{\Lambda_c p}^{1/2} \tilde{\lambda}_{\mathbb{S}\bar{\mathbb{S}}'}^{1/2}}{3(8\pi m_{\Lambda_c} \hat{s})^3} \left\{ \left[|\kappa_{\mathbb{S}\bar{\mathbb{S}}'}^{\mathbb{V}}|^2 (2\mathbf{F}_\perp^2 \hat{s} + \mathbf{F}_+^2 \mathbf{M}_+^2) \hat{\sigma}_- + |\kappa_{\mathbb{S}\bar{\mathbb{S}}'}^{\mathbb{A}}|^2 (2\mathbf{G}_\perp^2 \hat{s} + \mathbf{G}_+^2 \mathbf{M}_-^2) \hat{\sigma}_+ \right] \tilde{\lambda}_{\mathbb{S}\bar{\mathbb{S}}'} \right. \\ &+ 3|\kappa_{\mathbb{S}\bar{\mathbb{S}}'}^{\mathbb{V}} (m_{\mathbb{S}}^2 - m_{\mathbb{S}'}^2) + \kappa_{\mathbb{S}\bar{\mathbb{S}}'}^{\mathbb{S}} \hat{s}|^2 \hat{\sigma}_+ \mathbf{M}_-^2 \mathbf{F}_0^2 \\ &\left. + 3|\kappa_{\mathbb{S}\bar{\mathbb{S}}'}^{\mathbb{A}} (m_{\mathbb{S}'}^2 - m_{\mathbb{S}}^2) + \kappa_{\mathbb{S}\bar{\mathbb{S}}'}^{\mathbb{P}} \hat{s}|^2 \hat{\sigma}_- \mathbf{M}_+^2 \mathbf{G}_0^2 \right\}, \end{aligned} \quad (19)$$

where $\hat{\sigma}_\pm = \mathbf{M}_\pm^2 - \hat{s}$. It is to be integrated over $(m_{\mathbb{S}} + m_{\mathbb{S}'})^2 \leq \hat{s} \leq (m_{\Lambda_c} - m_p)^2$.

It is clear from eq. (19) that all of the four coefficients, $\kappa_{\mathbb{S}\bar{\mathbb{S}}'}^{\mathbb{S},\mathbb{P},\mathbb{V},\mathbb{A}}$, can be probed with this channel,⁵ unlike the mesonic cases of the previous subsections. However, it is worth pointing out that the $m_{\mathbb{S}} + m_{\mathbb{S}'}$ ranges that can be covered in the aforesaid baryonic modes are less than those in $D^0 \rightarrow (\gamma)\mathbb{S}\bar{\mathbb{S}}'$ and $\mathbb{D} \rightarrow \mathbb{P}\mathbb{S}\bar{\mathbb{S}}'$.

⁵ The expression in eq. (19) for $m_{\mathbb{S}} = m_{\mathbb{S}'}$ may be compared to the corresponding formula in ref. [51] for the rate of FCNC hyperon decay with invisible new bosons of equal mass in the final state.

III. NUMERICAL RESULTS FOR HADRON DECAYS INDUCED BY $c \rightarrow u\bar{S}\bar{S}'$

A. Constraints on effective couplings

As mentioned in section I, so far there have been only three attempts to look for FCNC $|\Delta C| = 1$ processes with missing energy and the null outcomes translated into caps on their branching fractions. The first two are $\mathcal{B}(D^0 \rightarrow \text{invisibles}) < 9.4 \times 10^{-5}$ and $\mathcal{B}(D^0 \rightarrow \pi^0 \nu \bar{\nu}) < 2.1 \times 10^{-4}$ both at 90% CL [28, 29]. Since the neutrinos in the second measurement were unobserved, we can apply these data to test the predictions for $D^0 \rightarrow \bar{S}\bar{S}'$ and $D^0 \rightarrow \pi^0 \bar{S}\bar{S}'$, respectively. The third finding, $\mathcal{B}(\Lambda_c^+ \rightarrow p\gamma') < 8.0 \times 10^{-5}$ at 90% CL [30], concerns a two-body decay with the missing energy carried away solely by a massless dark photon (γ') and therefore would not pertain directly to the Λ_c^+ three-body case under study. Nevertheless, the fact that BESIII has only recently acquired this bound indicates that it might in the near future also report its three-body counterpart, which would perhaps be comparable in order of magnitude.⁶ This implies that, for the following numerical exercise, it is reasonable to suppose that the Λ_c^+ result above is also the limit for the three-body mode, and consequently we may impose

$$\begin{aligned} \mathcal{B}(D^0 \rightarrow \bar{S}\bar{S}') &< 9.4 \times 10^{-5}, & \mathcal{B}(D^0 \rightarrow \pi^0 \bar{S}\bar{S}') &< 2.1 \times 10^{-4}, \\ \mathcal{B}(\Lambda_c^+ \rightarrow p\bar{S}\bar{S}') &< 8.0 \times 10^{-5}. \end{aligned} \tag{20}$$

For discussion purposes, we regard the third number on the same footing as the other two, while keeping in mind that it is only suggestive, being inspired by the $\Lambda_c^+ \rightarrow p\gamma'$ data.

Hereafter, we entertain the possibility that merely one of the couplings $\kappa_{\bar{S}\bar{S}'}^{V,A,S,P}$ is nonvanishing at a time, which simplifies the analysis. Moreover, accepting that \mathbf{S} and \mathbf{S}' can be nondegenerate, we include instances where $m_{S'} \neq m_S$. In numerical calculations, we employ the central values of $f_D = 212.0(7)$ MeV and the pertinent hadron lifetimes and masses from ref. [27] and the form factors specified in appendix A.

After implementing eq. (20), we extract the maximal magnitudes of the individual couplings versus $m_S + m_{S'}$. The outcomes are depicted in figure 2, where the blue, purple, and red curves correspond to the three limits in eq. (20), respectively. In each plot, the viable region for a particular $m_{S'}/m_S$ case is below the lower of the purple or blue and red curves.

This figure makes plain, as alluded to earlier, that $\Lambda_c^+ \rightarrow p\bar{S}\bar{S}'$ covers a narrower span of $m_S + m_{S'}$ than $D^0 \rightarrow \pi^0 \bar{S}\bar{S}'$ can, and certainly more so than $D^0 \rightarrow \bar{S}\bar{S}'$. Where the former two overlap in their mass coverage, we notice from the left portion of figure 2 that for $m_S + m_{S'} \lesssim 1$ GeV the values of $|\kappa_{\bar{S}\bar{S}'}^V|_{\max}$ and $|\kappa_{\bar{S}\bar{S}'}^S|_{\max}$ which are permitted by eq. (20) are roughly comparable in order of magnitude. By contrast, the top-right part of figure 2 reveals that $|\kappa_{\bar{S}\bar{S}'}^A|_{\max}$ inferred from the $D^0 \rightarrow \bar{S}\bar{S}'$ bound can be tremendously dissimilar to that from $\Lambda_c^+ \rightarrow p\bar{S}\bar{S}'$, depending on $m_S + m_{S'}$

⁶ With the data sample cited in ref. [30] the three-body bound would be relatively weaker due to a decreased detection efficiency, but fresh data to be collected in a few years might lead to a stronger bound not far from what we have adopted.

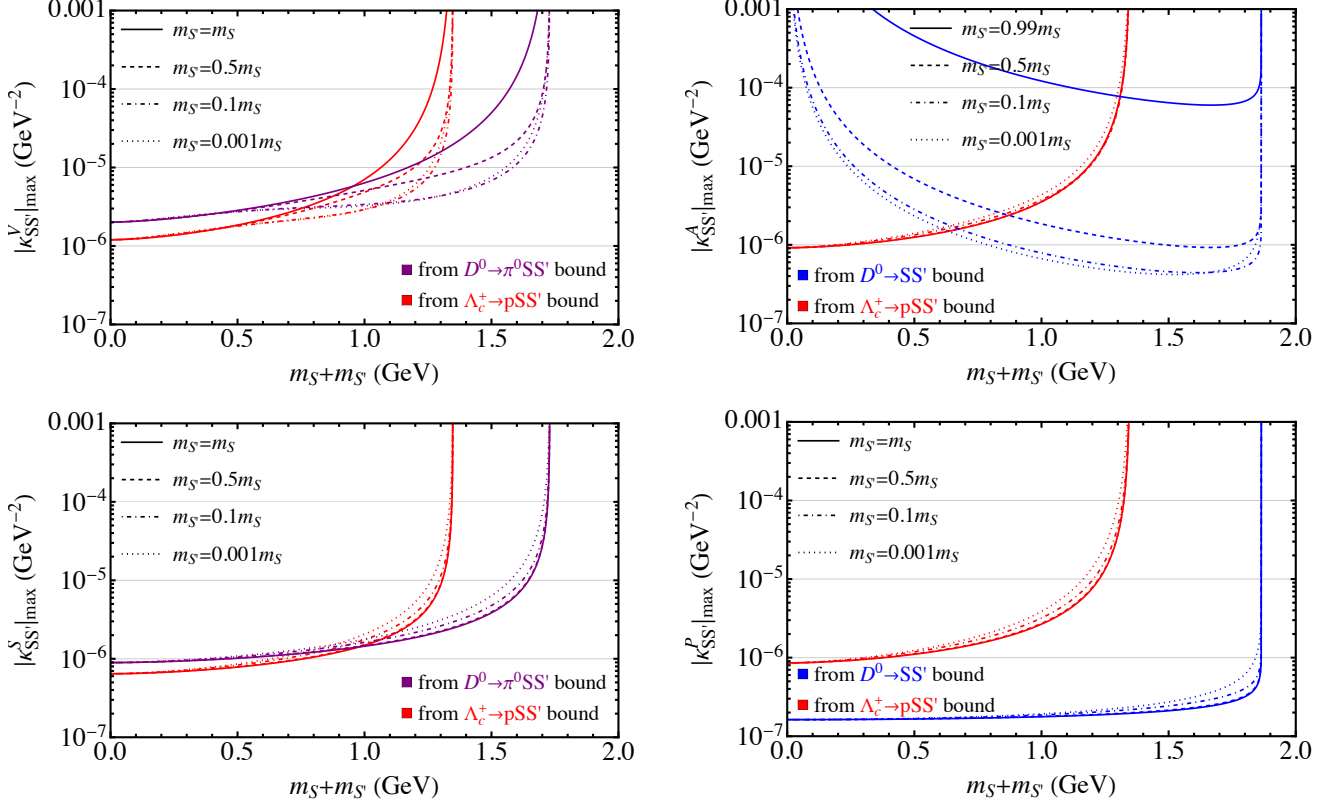


FIG. 2. The upper limits on $|\kappa_{SS'}^V|$ (top left), $|\kappa_{SS'}^A|$ (top right), $|\kappa_{SS'}^S|$ (bottom left), and $|\kappa_{SS'}^P|$ (bottom right) versus $m_S + m_{S'}$ obtained from the $D^0 \rightarrow S\bar{S}'$ (blue), $D^0 \rightarrow \pi^0 S\bar{S}'$ (purple), and $\Lambda_c^+ \rightarrow p S\bar{S}'$ (red) limits in eq. (20) for various $m_{S'}/m_S$ values if only one of $\kappa_{SS'}^{V,A,S,P}$ is nonzero at a time.

and $m_{S'}/m_S$, whereas the bottom-right graph shows that for $|\kappa_{SS'}^P|_{\max}$ the $\Lambda_c^+ \rightarrow p S\bar{S}'$ limit is not competitive to the $D^0 \rightarrow S\bar{S}'$ one. Furthermore, from the graphs in figure 2, we learn that the $|\kappa_{SS'}^S|_{\max}$ and $|\kappa_{SS'}^P|_{\max}$ curves and the red $|\kappa_{SS'}^A|_{\max}$ ones are not much affected by the choice of $m_{S'}/m_S$, the $|\kappa_{SS'}^V|_{\max}$ curves are moderately dependent on this ratio, and the blue $|\kappa_{SS'}^A|_{\max}$ ones manifest substantial variations with it. The upward trend exhibited by the blue $|\kappa_{SS'}^A|_{\max}$ curves in the top-right part of figure 2 as $m_{S'}$ approaches m_S of course reflects the loosening of the $D^0 \rightarrow S\bar{S}'$ restraint, as dictated by eq. (6). Accordingly, it is interesting to observe that presently $\kappa_{SS'}^A$ is not subject to any empirical bound if $m_S = m_{S'}$ and $m_S + m_{S'} > m_{\Lambda_c} - m_p \simeq 1.36$ GeV. On the other hand, there are still no experimental restrictions on $\kappa_{SS'}^V$ and $\kappa_{SS'}^S$ ($\kappa_{SS'}^P$) if $m_S + m_{S'}$ exceeds $m_{D^0} - m_{\pi^0} \simeq 1.73$ GeV ($m_{D^0} \simeq 1.86$ GeV) regardless of $m_{S'}/m_S$. Needless to say, the lack of constraints in the 1.36-1.86 GeV interval invites making the first effort to search for $D^0 \rightarrow \gamma \cancel{E}$.

B. Predictions

The caps on $|\kappa_{SS'}^{V,A,S,P}|$ can be turned into predictions for the maximal branching fractions of other FCNC charmed-hadron decays with $S\bar{S}'$ in the final states, again under the assumption that

only one of the coefficients is nonvanishing at a time. We have drawn the results with respect to $m_S + m_{S'}$ in figures 3-6, where we have used the same curve styles for the constraints in eq. (20) and the $m_{S'}/m_S$ choices as in the corresponding $|\kappa_{SS'}^{V,A,S,P}|_{\max}$ graphs in figure 2. As will be illustrated in the following figures, whether or not m_S and $m_{S'}$ are equal could significantly impact the decay rate, especially if $\kappa_{SS'}^A$ is the dominant coupling or sole one present. In each of the branching-fraction plots, as before, the viable area for every $m_{S'}/m_S$ case is below the lower of the purple or blue and red curves.

The two graphs in figure 3 reveal that $D^0 \rightarrow \gamma SS'$ currently has a branching fraction that is unconfined and hence could be quite sizable. More precisely, it is less than 10^{-5} for total masses of up to 1.5 GeV or so, but there is no limitation on it if $m_S + m_{S'} > m_{D^0} - m_{\pi^0}$ with at least $\kappa_{SS'}^V$ contributing or if both $m_S + m_{S'} > m_{\Lambda_c} - m_p$ and $m_S = m_{S'}$ with at least $\kappa_{SS'}^A \neq 0$. This condition will change if BESIII or Belle II pursues $D^0 \rightarrow \gamma \cancel{E}$ and establishes a bound on it, if no discovery is made. Any data on this channel would be greatly welcome.

From the left graphs in figure 4, it is evident that $\mathcal{B}(D^+ \rightarrow \pi^+ SS')_{\max} \sim 0.001$ over the whole kinematical range. This number is about $2\tau_{D^+}/\tau_{D^0} \sim 5$ times the $D^0 \rightarrow \pi^0 SS'$ one in eq. (20), as expected from approximate isospin symmetry. This relatively weak limit on the D^+ channel at the moment, especially for $m_{\Lambda_c} - m_p \lesssim m_S + m_{S'} < m_{D^+} - m_{\pi^+}$, encourages hunting $D^+ \rightarrow \pi^+ \cancel{E}$ as well.⁷ From the right column of figure 4, we see that $D_s^+ \rightarrow K^+ SS'$ not only covers a shorter range of $m_S + m_{S'}$ but also has a maximal branching-fraction which is comparatively smaller by several times or more. The latter observation might continue to be the rough pattern formed by the limits on $\mathbb{D} \rightarrow \mathbb{P} SS'$ from future quests. Nevertheless, if these decays are discovered, the acquired data can offer cross-checks on the effects of the responsible NP parametrized by $\kappa_{SS'}^{V,S}$.

From figure 5, it may be inferred that the $\mathbb{D} \rightarrow \mathbb{V} SS'$ channels have branching fractions which are further suppressed but can still reach roughly 1×10^{-4} . The situation resembles that of the

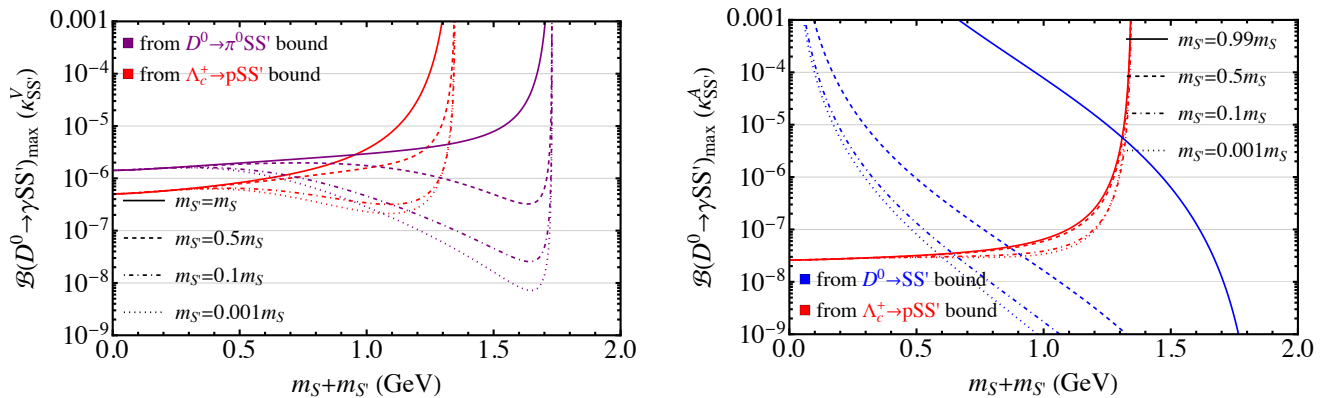


FIG. 3. The maximal branching fraction of $D^0 \rightarrow \gamma SS'$ due to $|\kappa_{SS'}^V|_{\max}$ (left) or $|\kappa_{SS'}^A|_{\max}$ (right) alone for various $m_{S'}/m_S$ choices.

⁷ The charged modes $D_{(s)}^+ \rightarrow \mathcal{M}_{(s)}^+ \cancel{E}$ with $\mathcal{M}_{(s)} = \pi, \rho(K, K^*)$ have backgrounds from the sequential decays $D_{(s)}^+ \rightarrow \tau^+ \nu$ and $\tau^+ \rightarrow \mathcal{M}_{(s)}^+ \bar{\nu}$ [2, 5], but we anticipate that they will be taken care of in the experimental searches.

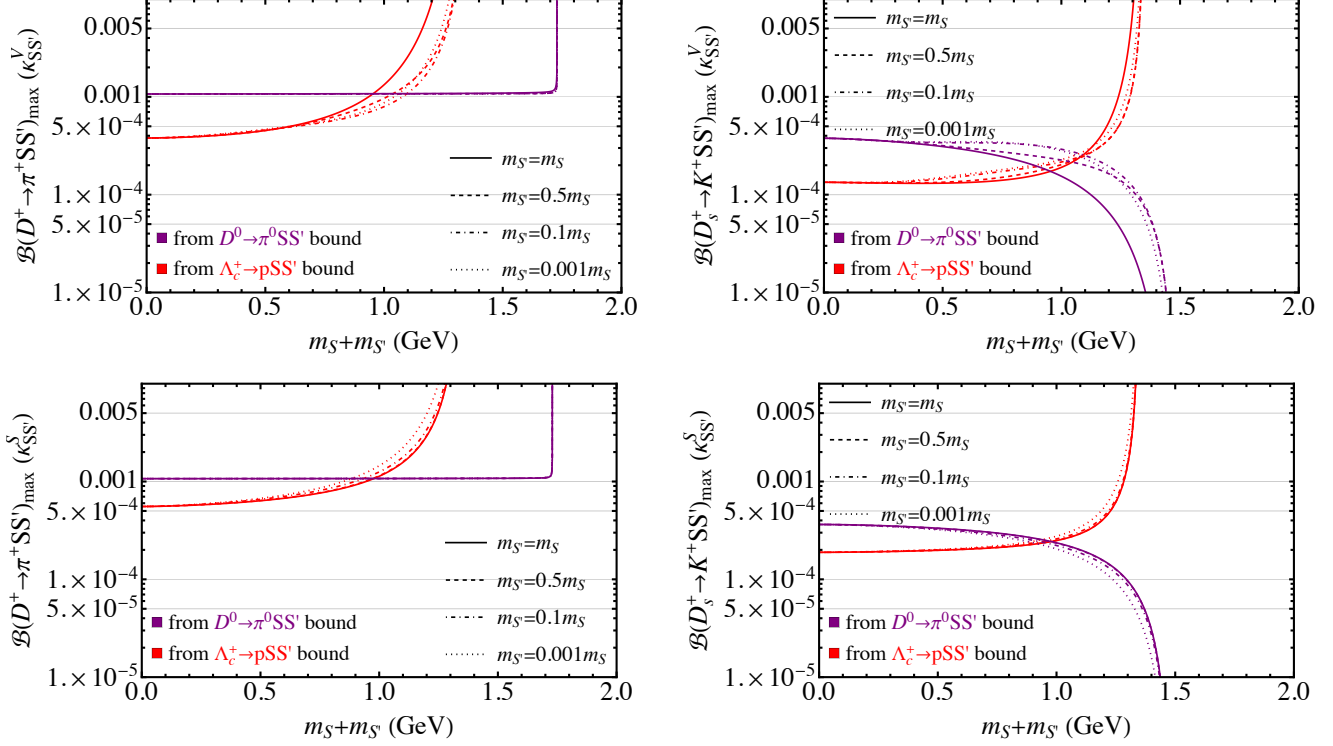


FIG. 4. The maximal branching fractions of $D^+ \rightarrow \pi^+ \bar{S} \bar{S}'$ (left column) and $D_s^+ \rightarrow K^+ \bar{S} \bar{S}'$ (right column) due to $|\kappa_{SS'}^V|_{\max}$ (top row) or $|\kappa_{SS'}^S|_{\max}$ (bottom row) alone for different $m_{S'}/m_S$ values.

charmed-baryon decays $\Xi_c^0 \rightarrow \Sigma^0 \bar{S} \bar{S}'$ and $\Xi_c^0 \rightarrow \Lambda \bar{S} \bar{S}'$, illustrated in figure 6, as well as $\Xi_c^+ \rightarrow \Sigma^+ \bar{S} \bar{S}'$, which has a branching fraction around $2\tau_{\Xi_c^+}/\tau_{\Xi_c^0} \sim 6$ times that of $\Xi_c^0 \rightarrow \Sigma^0 \bar{S} \bar{S}'$ but which is not included in the figure.

As a reminder, we remark that the red curves in our figures are only indicative for now, not being based on actual data on $\Lambda_c^+ \rightarrow p \bar{E}$ with two invisibles being emitted. Thus, empirical information on it would be highly desirable, as may also be concluded from the graphs we have produced. Importantly, this in addition means that the predicted upper-limits on branching fractions which we have discussed could be even bigger in the absence of the red curves. This is another incentive to look for these decay modes.

To demonstrate this more explicitly, as well as for completeness and reference, in Tables I and II we provide numerical examples of the maximal branching-fractions (the unbracketed entries in columns 2-4) for $m_S = m_{S'} = 0$ and $m_{S'} = 0.1 m_S = 0.05$ GeV, respectively, if the $\Lambda_c^+ \rightarrow p \bar{S} \bar{S}'$ bound is not present. When it is taken into account and the stronger, we obtain the numbers placed in brackets. It is worth noting that, as the third column of Table I makes clear, if $m_S = m_{S'} = 0$ and the $\Lambda_c^+ \rightarrow p \bar{S} \bar{S}'$ bound is dropped, the branching fractions of modes which get a contribution from $\kappa_{SS'}^A$ is currently unconfined and hence could be substantial.

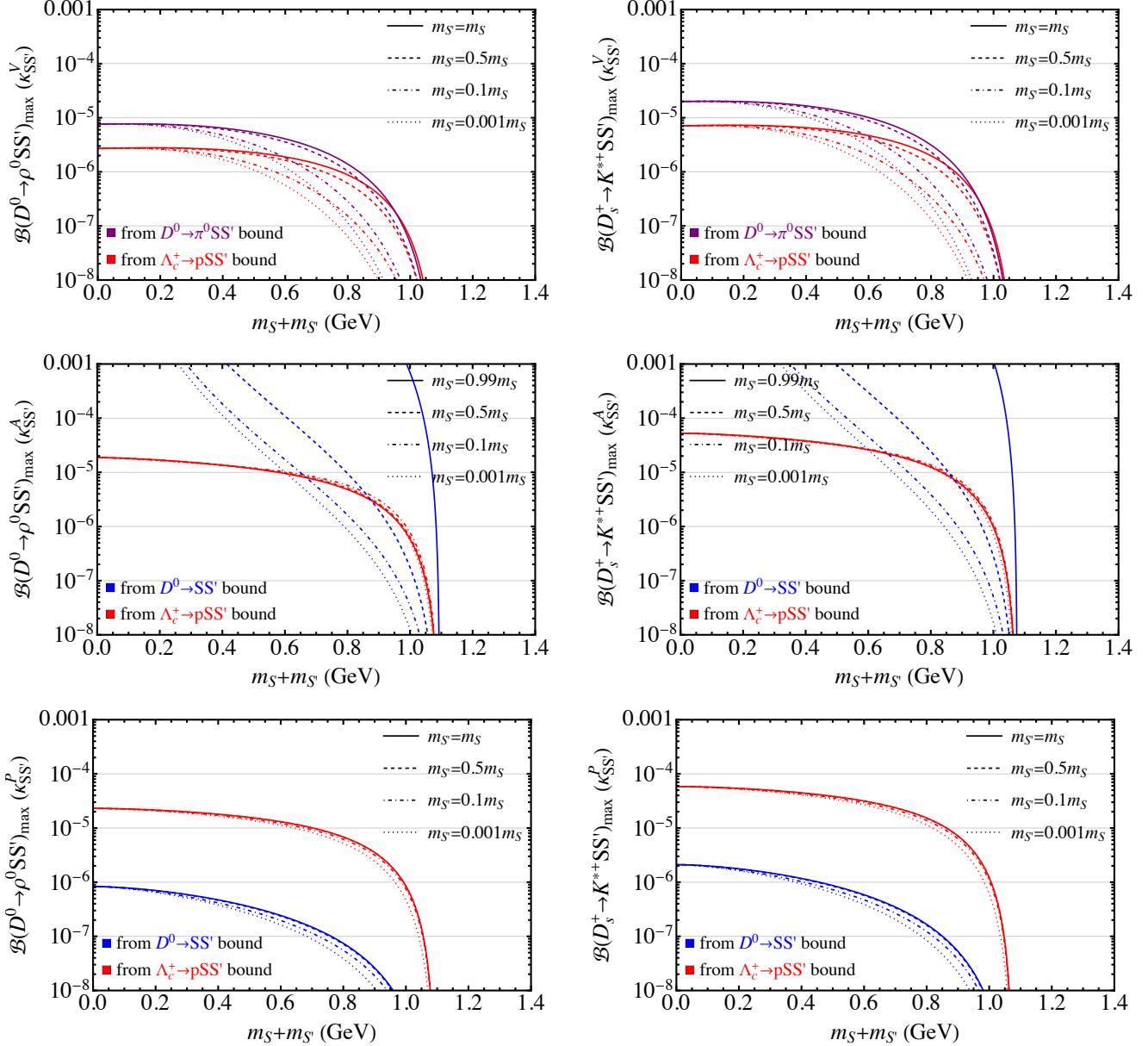


FIG. 5. The maximal branching fractions of $D^0 \rightarrow \rho^0 \bar{S}S'$ (left column) and $D_s^+ \rightarrow K^{*+} \bar{S}S'$ (right column) due to $|\kappa_{SS'}^V|_{\max}$ (top row) or $|\kappa_{SS'}^A|_{\max}$ (middle row) or $|\kappa_{SS'}^P|_{\max}$ (bottom row) alone. The $D^+ \rightarrow \rho^+ \bar{S}S'$ curves, not displayed, are approximately $2\tau_{D^+}/\tau_{D^0} \sim 5$ times their $D^0 \rightarrow \rho^0 \bar{S}S'$ counterparts.

IV. FCNC CHARM DECAY WITH INVISIBLE SINGLET FERMIONS

The possibility that the missing energy in $c \rightarrow u \cancel{E}$ is carried away by two SM-gauge-singlet spin-1/2 particles has been entertained in the past to varying extents [6–10]. Instead of adopting a model-independent approach as in the last two sections, here we consider a specific new-physics scenario where a heavy scalar leptoquark (LQ) is responsible for linking three Dirac right-handed sterile neutrinos (referred to as N_1, N_2, N_3), which are the singlet fermions, to up-type quarks which are also right-handed. This is the least constrained of the LQ models investigated in ref. [10] in the

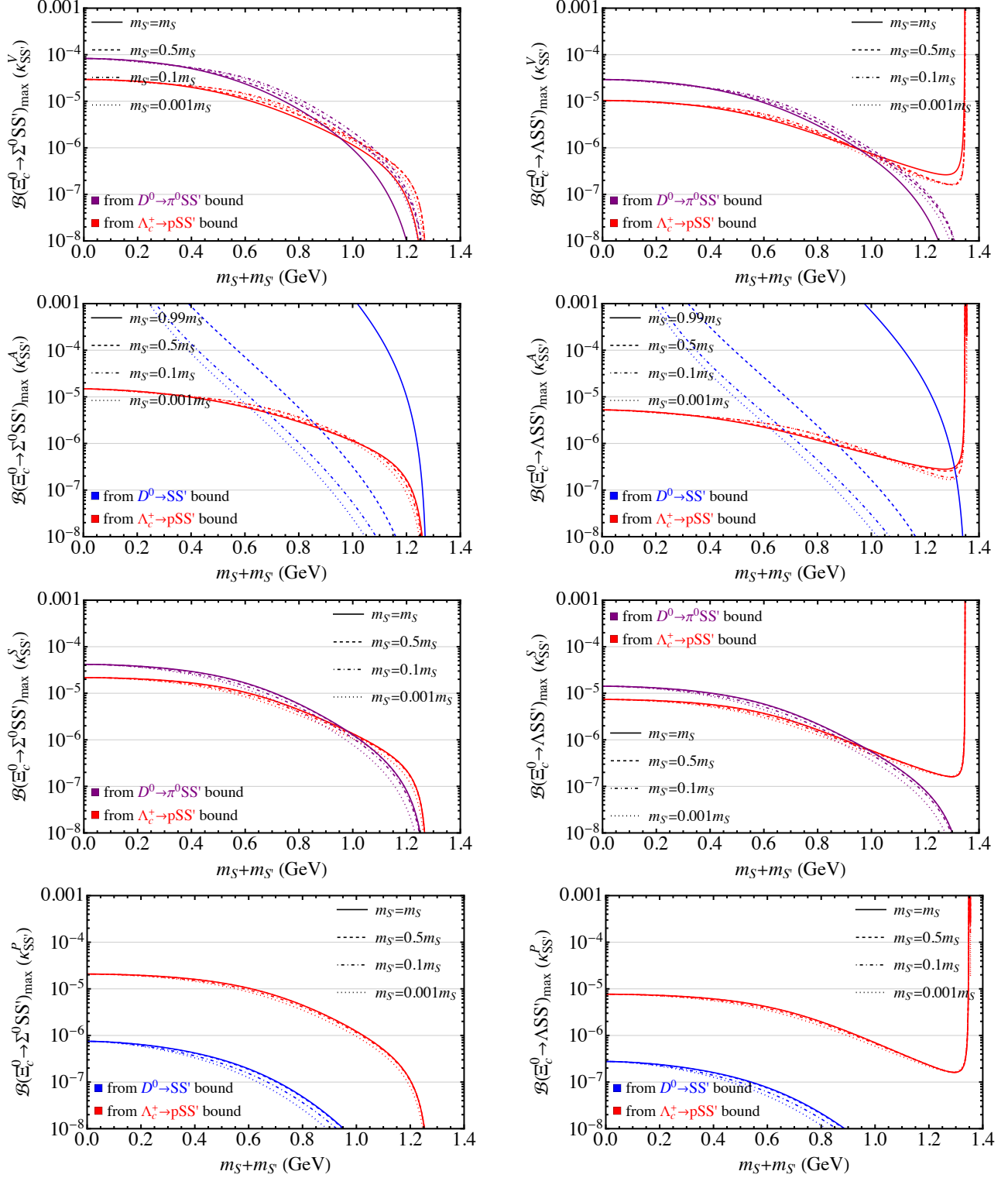


FIG. 6. The maximal branching fractions of $\Xi_c^0 \rightarrow \Sigma^0 \bar{S} S'$ (left column) and $\Xi_c^0 \rightarrow \Lambda \bar{S} S'$ (right column) due to $|\kappa_{SS'}^V|_{\max}$ (top row) or $|\kappa_{SS'}^A|_{\max}$ (second row) or $|\kappa_{SS'}^S|_{\max}$ (third row) or $|\kappa_{SS'}^P|_{\max}$ (bottom row) alone. The $\Xi_c^+ \rightarrow \Sigma^+ \bar{S} S'$ curves, not shown, are approximately $2\tau_{\Xi_c^+}/\tau_{\Xi_c^0} \sim 6$ times their $\Xi_c^0 \rightarrow \Sigma^0 \bar{S} S'$ counterparts.

TABLE I. The upper limits on branching fractions, in units of 10^{-5} , of various charmed-hadron decays induced by the $c \rightarrow u\bar{S}S'$ operators for $m_{S'} = m_S = 0$ if the $\Lambda_c^+ \rightarrow p\bar{S}S'$ bound is absent and, in brackets, if it is taken into account and the stronger. Only one of the coefficients $\kappa_{SS'}^{V,A,S,P}$ of the operators is taken to be nonzero at a time. A dash entry under $\kappa_{SS'}^X \neq 0$ means that $\kappa_{SS'}^X$ does not affect the decay.

Decay modes	$\kappa_{SS'}^V \neq 0$	$\kappa_{SS'}^A \neq 0$	$\kappa_{SS'}^S \neq 0$	$\kappa_{SS'}^P \neq 0$
$D^0 \rightarrow \bar{S}S'$	-	-	-	9.4 [Input]
$D^0 \rightarrow \gamma\bar{S}S'$	0.14 (0.050)	(0.0026)	-	-
$D^0 \rightarrow \pi^0\bar{S}S'$	21 [Input] (7.5)	-	21 [Input] (11)	-
$D^+ \rightarrow \pi^+\bar{S}S'$	107 (38)	-	107 (55)	-
$D_s^+ \rightarrow K^+\bar{S}S'$	38 (13)	-	36 (19)	-
$D^0 \rightarrow \rho^0\bar{S}S'$	0.74 (0.26)	(1.8)	-	0.081
$D^+ \rightarrow \rho^+\bar{S}S'$	3.8 (1.4)	(9.4)	-	0.42
$D_s^+ \rightarrow K^{*+}\bar{S}S'$	2.0 (0.71)	(5.3)	-	0.21
$\Lambda_c^+ \rightarrow p\bar{S}S'$	23 (8.0 [Input])	(8.0 [Input])	15 (8.0 [Input])	0.29
$\Xi_c^+ \rightarrow \Sigma^+\bar{S}S'$	49 (17)	(8.7)	25 (13)	0.44
$\Xi_c^0 \rightarrow \Sigma^0\bar{S}S'$	8.3 (2.9)	(1.5)	4.2 (2.2)	0.075
$\Xi_c^0 \rightarrow \Lambda\bar{S}S'$	2.9 (1.0)	(0.52)	1.4 (0.74)	0.028

TABLE II. The same as Table I but for $m_{S'} = 0.1 m_S = 0.05$ GeV.

Decay modes	$\kappa_{SS'}^V \neq 0$	$\kappa_{SS'}^A \neq 0$	$\kappa_{SS'}^S \neq 0$	$\kappa_{SS'}^P \neq 0$
$D^0 \rightarrow \bar{S}S'$	-	9.4 [Input] (3.5)	-	9.4 [Input]
$D^0 \rightarrow \gamma\bar{S}S'$	0.14 (0.063)	0.0081 (0.0030)	-	-
$D^0 \rightarrow \pi^0\bar{S}S'$	21 [Input] (9.3)	-	21 [Input] (13)	-
$D^+ \rightarrow \pi^+\bar{S}S'$	107 (47)	-	107 (68)	-
$D_s^+ \rightarrow K^+\bar{S}S'$	34 (15)	-	32 (20)	-
$D^0 \rightarrow \rho^0\bar{S}S'$	0.23 (0.10)	2.9 (1.1)	-	0.024
$D^+ \rightarrow \rho^+\bar{S}S'$	1.2 (0.55)	15 (5.6)	-	0.12
$D_s^+ \rightarrow K^{*+}\bar{S}S'$	0.62 (0.27)	8.1 (3.0)	-	0.060
$\Lambda_c^+ \rightarrow p\bar{S}S'$	18 (8.0 [Input])	22 (8.0 [Input])	13 (8.0 [Input])	0.14
$\Xi_c^+ \rightarrow \Sigma^+\bar{S}S'$	22 (9.9)	13 (4.7)	10 (6.5)	0.12
$\Xi_c^0 \rightarrow \Sigma^0\bar{S}S'$	3.8 (1.7)	2.2 (0.80)	1.7 (1.1)	0.020
$\Xi_c^0 \rightarrow \Lambda\bar{S}S'$	1.4 (0.61)	0.82 (0.30)	0.61 (0.39)	0.0078

$c \rightarrow u\cancel{E}$ context and can now be scrutinized to a greater degree in light of the recent Belle and BESIII data.

In the nomenclature of ref. [7], the LQ is \bar{S}_1 which transforms as $(\bar{3}, 1, -2/3)$ under the SM gauge groups $SU(3)_{\text{color}} \times SU(2)_L \times U(1)_Y$. We write the Lagrangian for the renormalizable interaction of \bar{S}_1 with $N_{1,2,3}$ and the quarks as

$$\mathcal{L}_{\text{LQ}} = \bar{Y}_{jl} \bar{U}_j^c P_R N_l \bar{S}_1 + \text{H.c.}, \quad (21)$$

where \bar{Y}_{jl} are generally complex elements of the LQ Yukawa matrix \bar{Y} , summation over family indices $j, l = 1, 2, 3$ is implicit, $\mathcal{U}_{1,2,3} = (u, c, t)$, and the superscript C indicates charge conjugation. Assuming the LQ to be heavy, we can then derive an effective Lagrangian of the form in eq. (B1) for $c \rightarrow uN\bar{N}'$, with the coefficients being given by

$$\mathbf{C}_{N_j N_l}^V = \mathbf{C}_{N_j N_l}^A = \tilde{\mathbf{C}}_{N_j N_l}^V = \tilde{\mathbf{C}}_{N_j N_l}^A = -\frac{\bar{Y}_{1j}^* \bar{Y}_{2l}}{8m_{\bar{S}_1}^2}. \quad (22)$$

As explained in ref. [10], the interactions in eq. (21) also bring about one-loop contributions to D^0 - \bar{D}^0 mixing which are proportional to the combination $\sum_j \bar{Y}_{1j}^* \bar{Y}_{2j} / m_{\bar{S}_1}$ and which therefore will vanish if the nonzero elements of the first and second rows of \bar{Y} do not share same columns. Hence the potentially stringent restrictions on the parameters of this model from D^0 - \bar{D}^0 mixing could be completely evaded. To realize this, for definiteness we choose, as one of the simplest examples,

$$\bar{Y} = \begin{pmatrix} 0 & \bar{y}_{u2} & 0 \\ \bar{y}_{c1} & 0 & 0 \\ 0 & 0 & 0 \end{pmatrix}, \quad (23)$$

in which case only $c \rightarrow uN_2\bar{N}_1$ can occur with

$$\mathbf{C}_{N_2 N_1}^V = \mathbf{C}_{N_2 N_1}^A = \tilde{\mathbf{C}}_{N_2 N_1}^V = \tilde{\mathbf{C}}_{N_2 N_1}^A = -\frac{\bar{y}_{u2}^* \bar{y}_{c1}}{8m_{\bar{S}_1}^2} \equiv \mathbf{K}_{NN'}, \quad (24)$$

the other coefficients vanishing.

Another empirical constraint, deduced from the latest LHC data, excludes at 95% CL scalar LQs having masses up to 1.14 TeV and decaying fully to a neutrino and a light-flavored quark [56]. Since this is applicable to \mathcal{L}_{LQ} , we select $m_{\bar{S}_1} > 1.2$ TeV. There is additionally a theoretical requirement for the elements of \bar{Y} , namely that their size not exceed $\sqrt{4\pi}$ to ensure perturbativity. It follows that $|\mathbf{K}_{NN'}| < 1.1 \text{ TeV}^{-2}$.

We now examine how the aforementioned Belle and BESIII measurements may test this particular case, with $\mathbf{K}_{NN'}$ and the masses of $N = N_2$ and $N' = N_1$ being the only free parameters. To begin, analogously to eq. (20) we impose

$$\begin{aligned} \mathcal{B}(D^0 \rightarrow N\bar{N}') &< 9.4 \times 10^{-5}, & \mathcal{B}(D^0 \rightarrow \pi^0 N\bar{N}') &< 2.1 \times 10^{-4}, \\ \mathcal{B}(\Lambda_c^+ \rightarrow p N\bar{N}') &< 8.0 \times 10^{-5}. \end{aligned} \quad (25)$$

Subsequently, after incorporating eq. (24) into the relevant rate formulas from eqs. (B2)-(B4) with the appropriate form factors from appendix A, we extract the maximal values of $|\mathbf{K}_{NN'}|$ over the permitted range of $m_N + m_{N'}$ for a few choices of $m_{N'}/m_N$. We display the results in figure 7, where the blue, purple, and red curves correspond, respectively, to the three limits in eq. (25). The allowed $|\mathbf{K}_{NN'}|$ range for each $(m_N, m_{N'})$ pair is below the lowest curve.

We learn from this figure that the restraints on $\mathbf{K}_{NN'}$ from $D^0 \rightarrow N\bar{N}'$ and $\Lambda_c^+ \rightarrow p N\bar{N}'$ in tandem are more stringent than the one from $D^0 \rightarrow \pi^0 N\bar{N}'$ and 3-4 times stronger than the one implied by

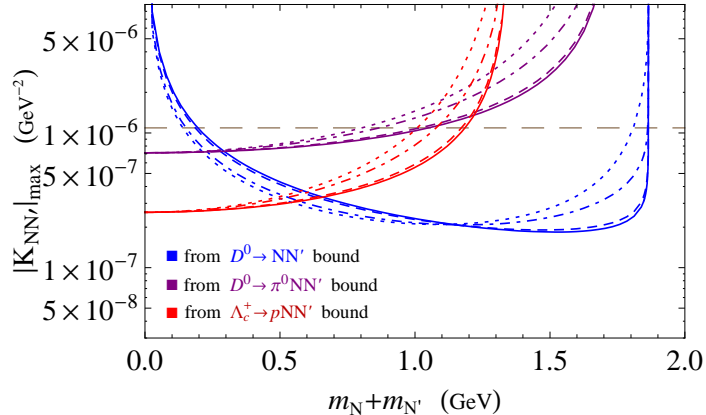


FIG. 7. The upper limits on $|\mathcal{K}_{\mathbb{N}\mathbb{N}'}|$ versus $m_{\mathbb{N}} + m_{\mathbb{N}'}$, with $\mathbb{N} = \mathbb{N}_2$ and $\mathbb{N}' = \mathbb{N}_1$, implied by the $D^0 \rightarrow \mathbb{N}\bar{\mathbb{N}'}$ (blue), $D^0 \rightarrow \pi^0 \mathbb{N}\bar{\mathbb{N}'}$ (purple), and $\Lambda_c^+ \rightarrow p \mathbb{N}\bar{\mathbb{N}'}$ (red) bounds in eq. (25) for $m_{\mathbb{N}'}/m_{\mathbb{N}} = 0.001$ (dotted curves), 0.1 (dash-dotted curves), 0.5 (dashed curves), 1 (solid curves). The horizontal brown dashed line marks $|\mathcal{K}_{\mathbb{N}\mathbb{N}'}| < 1.1 \text{ TeV}^{-2}$ inferred from collider and perturbativity restrictions.

collider data and perturbativity. We also notice that none of the sets of curves of the same color exhibit substantial variations with $m_{\mathbb{N}'}/m_{\mathbb{N}}$, and so there is no drastic weakening of the constraints when $m_{\mathbb{N}'} \rightarrow m_{\mathbb{N}}$, unlike the situation depicted by figure 2 in the invisible-boson case. This is mostly because of the difference in dependence on the invisibles' masses between the $D^0 \rightarrow \mathbb{N}\bar{\mathbb{N}'}$ rate and the $\kappa_{\mathbb{S}\mathbb{S}'}^A$ part of $\Gamma_{D^0 \rightarrow \mathbb{S}\bar{\mathbb{S}'}}$, as can be viewed in eqs. (B2) and (6). What we see in figure 7 again illustrates the importance of the mesonic and baryonic modes as complementary tools in the quest for new-physics signals.

A further comparison of figures 2 and 7 highlights one of the main differences between a model-independent analysis and a model-based one. In figure 2 the coefficients of the operators contributing to $c \rightarrow u \cancel{E}$ are taken to be independent of one another and consequently each have to respect only a subset of the pertinent data. By contrast, the coefficients described in figure 7, associated with the operators listed in eq. (B1), are connected via eq. (24), and the same $\mathcal{K}_{\mathbb{N}\mathbb{N}'}$ must satisfy all of the requisites in eq. (25), resulting by and large in a stronger restriction on it.

From the $|\mathcal{K}_{\mathbb{N}\mathbb{N}'}|_{\text{max}}$ values, we can predict the maximal branching-fractions of a number of hadron decays arising from the $c \rightarrow u \mathbb{N}\bar{\mathbb{N}'}$ operators. The results, plotted in figures 8 and 9, are on the whole lower than the corresponding ones in the scalar case, in figures 3-6, considering that the effects of the scalar coefficient $\kappa_{\mathbb{S}\mathbb{S}'}^A$, if $m_{\mathbb{S}} \simeq m_{\mathbb{S}'}$ are presently unknown and consequently could be sizable. Nevertheless, as figures 8 and 9 reveal, the predictions can still be significant, especially if $m_{\mathbb{N}} + m_{\mathbb{N}'} < 300 \text{ MeV}$ and the red curves are ignored. This is shown explicitly by the numerical examples quoted in table III, which may be compared with tables I and II. We can then conclude that this specific new-physics scenario remains alive and attractive, notably because it accommodates both a leptoquark and sterile neutrinos, and will be probed more thoroughly by future data.

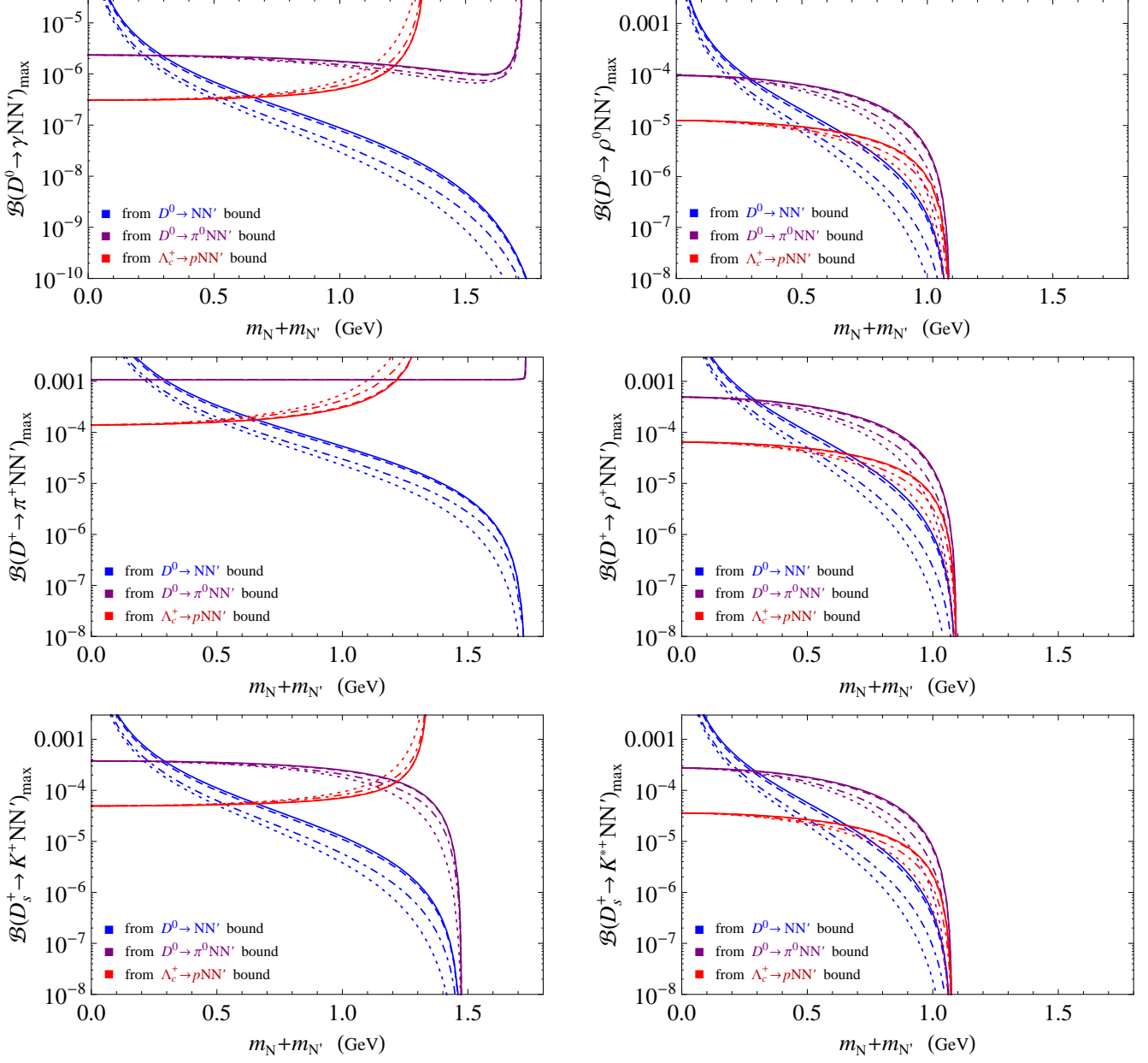


FIG. 8. Maximal branching fractions of $D^0 \rightarrow (\gamma, \rho^0)N\bar{N}'$, $D^+ \rightarrow (\pi^+, \rho^+)N\bar{N}'$, and $D_s^+ \rightarrow (K^+, K^{*+})N\bar{N}'$ translated from the $|K_{NN'}|_{\max}$ values in figure 7 inferred from the $D^0 \rightarrow N\bar{N}'$ (blue), $D^0 \rightarrow \pi^0 N\bar{N}'$ (purple), and $\Lambda_c^+ \rightarrow pN\bar{N}'$ (red) bounds in eq. (25).

V. CONCLUSION

We have explored the possibility that the FCNC decays of charmed hadrons with missing energy are enhanced by new physics affecting the $c \rightarrow u\cancel{E}$ transition, where the missing energy is carried away by either a couple of spinless bosons or a pair of spin-1/2 Dirac fermions, all of which are singlets under the SM gauge groups. We study how the outcomes of the latest hunts for $D^0 \rightarrow \cancel{E}$ by Belle and $D^0 \rightarrow \pi^0\cancel{E}$ and $\Lambda_c^+ \rightarrow p\cancel{E}$ by BESIII can lead to constraints on the underlying operators

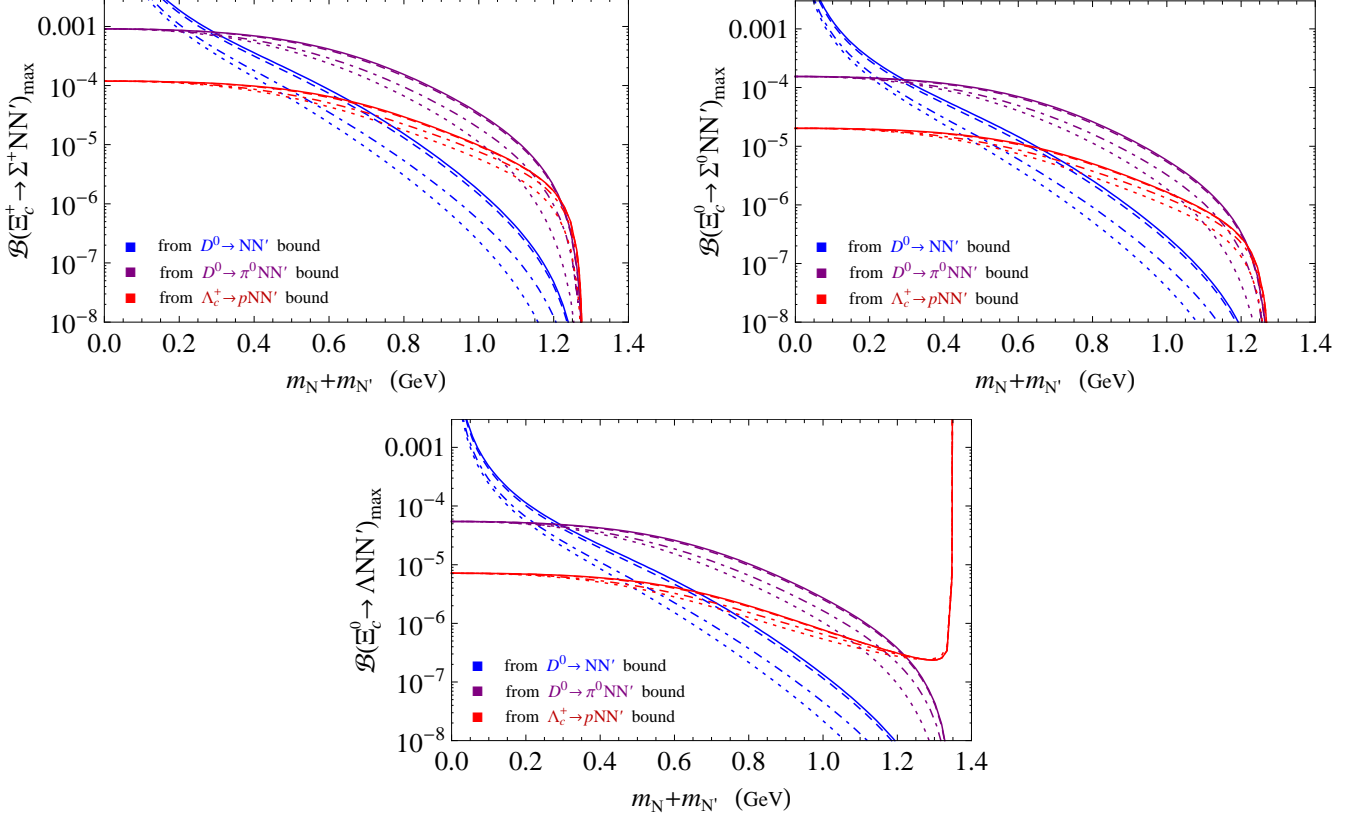


FIG. 9. The same as figure 8 but for $\Xi_c^{+,0} \rightarrow \Sigma^{+,0} \bar{N} \bar{N}'$ and $\Xi_c^0 \rightarrow \Lambda \bar{N} \bar{N}'$.

TABLE III. The upper limits on the branching fractions, in units of 10^{-5} , of various charmed-hadron decays induced by the $c \rightarrow u \bar{N} \bar{N}'$ interactions and evaluated with the lowest $|K_{NN'}|_{\max}$ for $m_{N'} = m_N = 0$ and $m_{N'} = 0.1 m_N = 0.05$ GeV if the $\Lambda_c^+ \rightarrow p \bar{N} \bar{N}'$ bound is absent and, in brackets, if it is included and the strongest.

Decay modes	$m_{N'} = m_N = 0$	$m_{N'} = 0.1 m_N = 0.05$ GeV
$D^0 \rightarrow \bar{N} \bar{N}'$	-	9.4 [Input]
$D^0 \rightarrow \gamma \bar{N} \bar{N}'$	0.15 (0.020)	0.021
$D^0 \rightarrow \pi^0 \bar{N} \bar{N}'$	21 [Input] (2.8)	3.1
$D^+ \rightarrow \pi^+ \bar{N} \bar{N}'$	107 (14)	16
$D_s^+ \rightarrow K^+ \bar{N} \bar{N}'$	38 (4.9)	4.9
$D^0 \rightarrow \rho^0 \bar{N} \bar{N}'$	9.6 (1.3)	0.68
$D^+ \rightarrow \rho^+ \bar{N} \bar{N}'$	49 (6.4)	3.5
$D_s^+ \rightarrow K^{*+} \bar{N} \bar{N}'$	27 (3.6)	1.9
$\Lambda_c^+ \rightarrow p \bar{N} \bar{N}'$	61 (8.0 [Input])	7.2
$\Xi_c^+ \rightarrow \Sigma^+ \bar{N} \bar{N}'$	91 (12)	5.4
$\Xi_c^0 \rightarrow \Sigma^0 \bar{N} \bar{N}'$	15 (2.0)	0.91
$\Xi_c^0 \rightarrow \Lambda \bar{N} \bar{N}'$	5.5 (0.71)	0.34

describing $c \rightarrow u\cancel{E}$. We demonstrate in our numerical work that these mesonic and baryonic modes already play valuable complementary roles in probing the operators. Yet, additional data on these decays are needed to improve on the existing empirical bounds, which are not yet very stringent. Moreover, other channels are also important to search for because they could provide extra means to restrain the potential new physics. Of great interest among them is $D^0 \rightarrow \gamma\cancel{E}$, which could still have a substantial branching fraction and covers the mass ranges of the invisible particles more than most of the other modes can. However, the latter channels, such as $D \rightarrow \rho\cancel{E}$ and $\Xi_c \rightarrow \Sigma\cancel{E}$, are of consequence as well, with branching fractions that are not very small. Many of the predictions we have made are expectedly testable by BESIII and Belle II in the near future

VI. ACKNOWLEDGMENTS

We thank Cong Geng and Yu Liu for information on experimental matters. JT thanks the Tsung-Dao Lee Institute, Shanghai Jiao Tong University, and the Hangzhou Institute for Advanced Study, University of Chinese Academy of Sciences, for their hospitality during the course of this work. It was supported in part by the National Key Research and Development Program of China under Grant No. 2020YFC2201501 and the National Natural Science Foundation of China (NSFC) under Grant No. 12147103 and No. 12247160.

Appendix A: Form factors in matrix elements of $c \rightarrow u$ currents

The form factors F_V and F_A for the $D^0 \rightarrow \gamma$ transition in eq. (8) have been addressed in the literature [1, 6, 57]. We employ the formulas from ref. [57]

$$F_V = \frac{(2/3)(-0.49)}{1 - \hat{q}^2/(2.0 \text{ GeV})^2}, \quad F_A = \frac{(2/3)(-0.17)}{1 - \hat{q}^2/(2.3 \text{ GeV})^2}, \quad (\text{A1})$$

which are functions of the squared momentum-transfer \hat{q}^2 .

In the remainder of this appendix, we rely on isospin symmetry to relate the hadronic matrix elements of the $c \rightarrow u$ bilinears to those of $c \rightarrow d$ in the references cited. One of the implications is that the form factors of $D^0 \rightarrow \pi^0(\rho^0)$ are $1/\sqrt{2}$ times the corresponding ones of $D^+ \rightarrow \pi^+(\rho^+)$ and those of $\Xi_c^0 \rightarrow \Sigma^0$ are $1/\sqrt{2}$ times their $\Xi_c^+ \rightarrow \Sigma^+$ counterparts.

For f_+ and f_0 in the $\mathbb{D} \rightarrow \mathbb{P}$ matrix elements defined by eq. (12), we adopt the lattice-QCD results of ref. [58] for $D \rightarrow \pi$ and $D_s \rightarrow K$ decays. The dependence of $f_{+,0}$ on \hat{q}^2 is given by [58]

$$f_+ = \frac{1}{1 - \hat{q}^2/(2.00685 \text{ GeV})^2} \sum_{n=0}^3 a_n \left[z^n - \frac{n z^4}{4(-1)^{4-n}} \right], \quad f_0 = \frac{1}{1 - \hat{q}^2/(2.3 \text{ GeV})^2} \sum_{n=0}^3 b_n z^n, \\ z = \frac{\sqrt{(M_D + M_\pi)^2 - \hat{q}^2} - M_D - M_\pi}{\sqrt{(M_D + M_\pi)^2 - \hat{q}^2} + M_D + M_\pi}, \quad M_D = 1864.83 \text{ MeV}, \quad M_\pi = 134.9768 \text{ MeV}, \quad (\text{A2})$$

where for $D^+ \rightarrow \pi^+$

$$a_0 = b_0 = 0.63, \quad a_1 = -0.61, \quad a_2 = -0.2, \quad a_3 = 0.3, \quad b_1 = 0.33, \quad b_2 = -0.31, \quad b_3 = -1.9 \quad (\text{A3})$$

and for $D_s^+ \rightarrow K^+$

$$a_0 = b_0 = 0.6307, \quad a_1 = -0.562, \quad a_2 = -0.19, \quad a_3 = 0.33, \quad b_1 = 0.347, \quad b_2 = 0.44, \quad b_3 = -0.21. \quad (\text{A4})$$

Concerning the $\mathbb{D} \rightarrow \mathbb{V}$ form factors $A_{0,1,2}$ and V in eq. (13), to our knowledge there are as yet no lattice computations of them. Therefore, we opt for the outcomes of a so-called symmetry-preserving formulation of a vector-vector contact interaction quite recently implemented in ref. [59], which have the form

$$\mathbb{F}(\hat{\mathbb{F}}_0, \hat{\mathbb{A}}, \hat{\mathbb{B}}) = \frac{\hat{\mathbb{F}}_0}{1 - \hat{\mathbb{A}} \hat{q}^2/m_P^2 + \hat{\mathbb{B}} (\hat{q}^2/m_P^2)^2}, \quad (\text{A5})$$

where $\hat{\mathbb{F}}_0$, $\hat{\mathbb{A}}$, $\hat{\mathbb{B}}$, and m_P are numbers obtained therein. Thus, for $D^+ \rightarrow \rho^+$

$$\begin{aligned} A_0 &= \mathbb{F}(0.61, 1.29, 0.27), & A_1 &= \mathbb{F}(0.52, 0.15, -0.14), & A_2 &= \mathbb{F}(0.36, 0.6, -0.042), \\ V &= \mathbb{F}(0.83, 0.87, 0.0009), & m_P &= 1.87 \text{ GeV} \end{aligned} \quad (\text{A6})$$

and for $D_s^+ \rightarrow K^{*+}$

$$\begin{aligned} A_0 &= \mathbb{F}(0.62, 1.4, 0.27), & A_1 &= \mathbb{F}(0.56, 0.22, -0.2), & A_2 &= \mathbb{F}(0.4, 0.72, -0.047), \\ V &= \mathbb{F}(0.94, 0.98, -0.0011), & m_P &= 1.96 \text{ GeV}. \end{aligned} \quad (\text{A7})$$

For $\mathbf{F}_{\perp,+0}$ and $\mathbf{G}_{\perp,+0}$ in the $\Lambda_c^+ \rightarrow p$ matrix elements given by eq. (17), we use the lattice-QCD results of ref. [60] which are parametrized as

$$\tilde{\mathbb{F}}(A_0, A_1, A_2) = \frac{A_0 + A_1 \tilde{z} + A_2 \tilde{z}^2}{1 - \hat{q}^2/m_{\text{pole}}^2}, \quad \tilde{z} = \frac{\sqrt{\tilde{\mathfrak{t}}_+ - \hat{q}^2} - \sqrt{\tilde{\mathfrak{t}}_+ - (m_{\Lambda_c} - m_N)^2}}{\sqrt{\tilde{\mathfrak{t}}_+ - \hat{q}^2} + \sqrt{\tilde{\mathfrak{t}}_+ - (m_{\Lambda_c} - m_N)^2}}, \quad (\text{A8})$$

where $\tilde{\mathfrak{t}}_+ = (1.87 + 0.135)^2 \text{ GeV}^2$ and m_N is the average nucleon mass. Accordingly, we have [60]

$$\begin{aligned} \mathbf{F}_{\perp} &= \tilde{\mathbb{F}}(1.36, -1.7, 0.71), & \mathbf{F}_{+} &= \tilde{\mathbb{F}}(0.83, -2.33, 8.41), & \mathbf{F}_0 &= \tilde{\mathbb{F}}(0.84, -2.57, 9.87), \\ \mathbf{G}_{\perp} &= \tilde{\mathbb{F}}(0.69, -0.68, 0.7), & \mathbf{G}_{+} &= \tilde{\mathbb{F}}(0.69, -0.9, 2.25), & \mathbf{G}_0 &= \tilde{\mathbb{F}}(0.73, -0.97, 0.83), \end{aligned} \quad (\text{A9})$$

with $m_{\text{pole}} = 2.01 \text{ GeV}$ for $\mathbf{F}_{\perp,+}$, 2.351 GeV for \mathbf{F}_0 , 2.423 GeV for $\mathbf{G}_{\perp,+}$, 1.87 GeV for \mathbf{G}_0 . We note that, instead of eq. (17), one can alternatively write

$$\begin{aligned} \langle p | \bar{u} \gamma^\mu c | \Lambda_c^+ \rangle &= \bar{u}_p \left(\gamma^\mu f_1 + \frac{[\gamma^\mu, \gamma^\omega] \hat{q}_\omega}{2m_{\Lambda_c}} f_2 + \frac{\hat{q}^\mu}{m_{\Lambda_c}} f_3 \right) u_{\Lambda_c}, \\ \langle p | \bar{u} \gamma^\mu \gamma_5 c | \Lambda_c^+ \rangle &= \bar{u}_p \left(\gamma^\mu g_1 + \frac{[\gamma^\mu, \gamma^\omega] \hat{q}_\omega}{2m_{\Lambda_c}} g_2 + \frac{\hat{q}^\mu}{m_{\Lambda_c}} g_3 \right) \gamma_5 u_{\Lambda_c}, \end{aligned} \quad (\text{A10})$$

where $f_{1,2,3}$ and $g_{1,2,3}$ are connected to $F_{\perp,+0}$ and $G_{\perp,+0}$ by

$$\begin{aligned} F_{\perp} &= f_1 + \frac{M_+ f_2}{m_{\Lambda_c}}, & F_+ &= f_1 + \frac{\hat{q}^2 f_2}{m_{\Lambda_c} M_+}, & F_0 &= f_1 + \frac{\hat{q}^2 f_3}{m_{\Lambda_c} M_-}, \\ G_{\perp} &= g_1 - \frac{M_- g_2}{m_{\Lambda_c}}, & G_+ &= g_1 - \frac{\hat{q}^2 g_2}{m_{\Lambda_c} M_-}, & G_0 &= g_1 - \frac{\hat{q}^2 g_3}{m_{\Lambda_c} M_+}. \end{aligned} \quad (\text{A11})$$

With regard to $\Xi_c \rightarrow \Sigma, \Lambda$, there is still no lattice analysis on their form factors as far as we can tell. Hence we adopt those estimated in ref. [61] in the light-front constituent quark model, which are expressible as $f_{1,2,3}$ and $g_{1,2,3}$, defined analogously to their $\Lambda_c^+ \rightarrow p$ counterparts in eq. (A10) and having the form $\tilde{F}(\kappa_0, \kappa_1, \kappa_2) = \kappa_0 / (1 - \kappa_1 \hat{q}^2 + \kappa_2 \hat{q}^4)$, with $\kappa_{0,1,2}$ being constants calculated therein. Thus, for $\Xi_c^+ \rightarrow \Sigma^+$

$$\begin{aligned} f_1 &= \tilde{F}(0.73, 1.49, 2.35), & f_2 &= \tilde{F}(0.99, 1.43, 2.38), \\ g_1 &= \tilde{F}(0.63, 1.18, 1.79), & g_2 &= \tilde{F}(0.11, 1.88, 2.88) \end{aligned} \quad (\text{A12})$$

and for $\Xi_c^0 \rightarrow \Lambda$

$$\begin{aligned} f_1 &= \tilde{F}(0.28, 1.5, 2.32), & f_2 &= \tilde{F}(0.38, 1.35, 2.3), \\ g_1 &= \tilde{F}(0.25, 1.18, 1.77), & g_2 &= \tilde{F}(0.04, 1.71, 2.78), \end{aligned} \quad (\text{A13})$$

but $f_3 = g_3 = 0$ in the formalism of ref. [61].

Appendix B: Predictions of the standard model

Before dealing with the SM case, we consider the more general, effective couplings of invisible spin-1/2 Dirac fermion fields \mathbf{f} and \mathbf{f}' to vector and axialvector $c \rightarrow u$ currents described by

$$\mathcal{L}_{\mathbf{f}\mathbf{f}'} = -\bar{u}\gamma^\mu c \bar{\mathbf{f}}\gamma_\mu (\mathbf{C}_{\mathbf{f}\mathbf{f}'}^{\mathbf{V}} + \gamma_5 \mathbf{C}_{\mathbf{f}\mathbf{f}'}^{\mathbf{A}}) \mathbf{f}' - \bar{u}\gamma^\mu \gamma_5 c \bar{\mathbf{f}}\gamma_\mu (\tilde{\mathbf{C}}_{\mathbf{f}\mathbf{f}'}^{\mathbf{V}} + \gamma_5 \tilde{\mathbf{C}}_{\mathbf{f}\mathbf{f}'}^{\mathbf{A}}) \mathbf{f}', \quad (\text{B1})$$

where the constants $\mathbf{C}_{\mathbf{f}\mathbf{f}'}^{\mathbf{V},\mathbf{A}}$ and $\tilde{\mathbf{C}}_{\mathbf{f}\mathbf{f}'}^{\mathbf{V},\mathbf{A}}$ may be complex. It will induce $D^0 \rightarrow \gamma \mathbf{f} \bar{\mathbf{f}}'$, $\mathbb{D} \rightarrow \mathbb{P} \mathbf{f} \bar{\mathbf{f}}'$, $\mathbb{V} \mathbf{f} \bar{\mathbf{f}}'$, and $\Lambda_c^+ \rightarrow p \mathbf{f} \bar{\mathbf{f}}'$ if kinematically allowed. The amplitudes for these decays can be derived after applying the hadronic matrix elements detailed in sections II A-II D to the quark bilinears in $\mathcal{L}_{\mathbf{f}\mathbf{f}'}$. Permitting $m_{\mathbf{f}}$ and $m_{\mathbf{f}'}$ to be unequal, we then arrive at the (differential) rates

$$\Gamma_{D^0 \rightarrow \gamma \mathbf{f} \bar{\mathbf{f}}'} = \frac{\lambda^{1/2}(m_{D^0}^2, m_{\mathbf{f}}^2, m_{\mathbf{f}'}^2)}{8\pi m_{D^0}^3} \left[|\tilde{\mathbf{C}}_{\mathbf{f}\mathbf{f}'}^{\mathbf{V}}|^2 (m_{D^0}^2 - \tilde{\mu}_+^2) \tilde{\mu}_-^2 + |\tilde{\mathbf{C}}_{\mathbf{f}\mathbf{f}'}^{\mathbf{A}}|^2 (m_{D^0}^2 - \tilde{\mu}_-^2) \tilde{\mu}_+^2 \right] f_D^2, \quad (\text{B2})$$

$$\frac{d\Gamma_{D^0 \rightarrow \gamma \mathbf{f} \bar{\mathbf{f}}'}}{d\hat{s}} = \frac{\alpha_e \tilde{\lambda}_{\mathbf{f}\mathbf{f}'}^{1/2} (m_{D^0}^2 - \hat{s})^3}{192\pi^2 m_{D^0}^5 \hat{s}^2} \left[\left(|\mathbf{C}_{\mathbf{f}\mathbf{f}'}^{\mathbf{V}}|^2 F_V^2 + |\tilde{\mathbf{C}}_{\mathbf{f}\mathbf{f}'}^{\mathbf{V}}|^2 F_A^2 \right) (3\hat{s} - \tilde{s}_+) \tilde{s}_- + \left(|\mathbf{C}_{\mathbf{f}\mathbf{f}'}^{\mathbf{A}}|^2 F_V^2 + |\tilde{\mathbf{C}}_{\mathbf{f}\mathbf{f}'}^{\mathbf{A}}|^2 F_A^2 \right) (3\hat{s} - \tilde{s}_-) \tilde{s}_+ \right],$$

$$\frac{d\Gamma_{\mathbb{D} \rightarrow \mathbb{P} \mathbf{f} \bar{\mathbf{f}}'}}{d\hat{s}} = \frac{4 \tilde{\lambda}_{\mathbb{D}\mathbb{P}}^{1/2} \tilde{\lambda}_{\mathbf{f}\mathbf{f}'}^{1/2}}{3(8\pi m_{\mathbb{D}} \hat{s})^3} \left\{ \left[|\mathbf{C}_{\mathbf{f}\mathbf{f}'}^{\mathbf{V}}|^2 (3\hat{s} - \tilde{s}_+) \tilde{s}_- + |\mathbf{C}_{\mathbf{f}\mathbf{f}'}^{\mathbf{A}}|^2 (3\hat{s} - \tilde{s}_-) \tilde{s}_+ \right] \tilde{\lambda}_{\mathbb{D}\mathbb{P}} F_+^2 + 3 \left(|\mathbf{C}_{\mathbf{f}\mathbf{f}'}^{\mathbf{V}}|^2 \tilde{\mu}_-^2 \tilde{s}_+ + |\mathbf{C}_{\mathbf{f}\mathbf{f}'}^{\mathbf{A}}|^2 \tilde{\mu}_+^2 \tilde{s}_- \right) F_0^2 m_+^2 m_-^2 \right\}, \quad (\text{B3})$$

$$\begin{aligned}
\frac{d\Gamma_{\mathbb{D} \rightarrow \mathbb{V} \mathbf{f} \mathbf{f}'}}{d\hat{s}} &= \frac{4 \tilde{\lambda}_{\mathbb{D}\mathbb{V}}^{3/2} \tilde{\lambda}_{\mathbf{f}\mathbf{f}'}^{1/2}}{(8\pi m_{\mathbb{D}} \hat{s})^3} \left\{ \left[|\mathbf{C}_{\mathbf{f}\mathbf{f}'}^{\mathbb{V}}|^2 (3\hat{s} - \tilde{s}_+) \tilde{s}_- + |\mathbf{C}_{\mathbf{f}\mathbf{f}'}^{\mathbb{A}}|^2 (3\hat{s} - \tilde{s}_-) \tilde{s}_+ \right] \frac{2\hat{s}V^2}{3\tilde{\mathbf{m}}_+^2} \right. \\
&\quad + \left[\frac{A_1^2 \tilde{\mathbf{m}}_+^2}{6m_{\mathbb{V}}^2} \left(\frac{1}{2} + \frac{6m_{\mathbb{V}}^2 \hat{s}}{\tilde{\lambda}_{\mathbb{D}\mathbb{V}}} \right) + \frac{\tilde{\lambda}_{\mathbb{D}\mathbb{V}} A_2^2}{12\tilde{\mathbf{m}}_+^2 m_{\mathbb{V}}^2} + \frac{\hat{s} - \tilde{\mathbf{m}}_+ \tilde{\mathbf{m}}_-}{6m_{\mathbb{V}}^2} A_1 A_2 \right] \\
&\quad \times \left[|\tilde{\mathbf{C}}_{\mathbf{f}\mathbf{f}'}^{\mathbb{V}}|^2 (3\hat{s} - \tilde{s}_+) \tilde{s}_- + |\tilde{\mathbf{C}}_{\mathbf{f}\mathbf{f}'}^{\mathbb{A}}|^2 (3\hat{s} - \tilde{s}_-) \tilde{s}_+ \right] \\
&\quad \left. + \left(|\tilde{\mathbf{C}}_{\mathbf{f}\mathbf{f}'}^{\mathbb{V}}|^2 \tilde{\mu}_-^2 \tilde{s}_+ + |\tilde{\mathbf{C}}_{\mathbf{f}\mathbf{f}'}^{\mathbb{A}}|^2 \tilde{\mu}_+^2 \tilde{s}_- \right) A_0^2 \right\}, \\
\frac{d\Gamma_{\Lambda_c^+ \rightarrow p \mathbf{f} \mathbf{f}'}}{d\hat{s}} &= \frac{4 \tilde{\lambda}_{\Lambda_c p}^{1/2} \tilde{\lambda}_{\mathbf{f}\mathbf{f}'}^{1/2}}{3(8\pi m_{\Lambda_c} \hat{s})^3} \left\{ \left[|\mathbf{C}_{\mathbf{f}\mathbf{f}'}^{\mathbb{V}}|^2 (3\hat{s} - \tilde{s}_+) \tilde{s}_- + |\mathbf{C}_{\mathbf{f}\mathbf{f}'}^{\mathbb{A}}|^2 (3\hat{s} - \tilde{s}_-) \tilde{s}_+ \right] (2f_{\perp}^2 \hat{s} + f_+^2 M_+^2) \hat{\sigma}_- \right. \\
&\quad + 3 \left(|\mathbf{C}_{\mathbf{f}\mathbf{f}'}^{\mathbb{V}}|^2 \tilde{\mu}_-^2 \tilde{s}_+ + |\mathbf{C}_{\mathbf{f}\mathbf{f}'}^{\mathbb{A}}|^2 \tilde{\mu}_+^2 \tilde{s}_- \right) \hat{\sigma}_+ f_0^2 M_+^2 \\
&\quad + \left[|\tilde{\mathbf{C}}_{\mathbf{f}\mathbf{f}'}^{\mathbb{V}}|^2 (3\hat{s} - \tilde{s}_+) \tilde{s}_- + |\tilde{\mathbf{C}}_{\mathbf{f}\mathbf{f}'}^{\mathbb{A}}|^2 (3\hat{s} - \tilde{s}_-) \tilde{s}_+ \right] (2g_{\perp}^2 \hat{s} + g_+^2 M_+^2) \hat{\sigma}_+ \\
&\quad \left. + 3 \left(|\tilde{\mathbf{C}}_{\mathbf{f}\mathbf{f}'}^{\mathbb{V}}|^2 \tilde{\mu}_-^2 \tilde{s}_+ + |\tilde{\mathbf{C}}_{\mathbf{f}\mathbf{f}'}^{\mathbb{A}}|^2 \tilde{\mu}_+^2 \tilde{s}_- \right) \hat{\sigma}_- g_0^2 M_+^2 \right\}, \tag{B4}
\end{aligned}$$

where

$$\begin{aligned}
\tilde{\mu}_{\pm} &= m_{\mathbf{f}} \pm m_{\mathbf{f}'}, & \mathbf{m}_{\pm} &= m_{\mathbb{D}} \pm m_{\mathbb{P}}, & \mathbf{M}_{\pm} &= m_{\Lambda_c} \pm m_p, \\
\tilde{s}_{\pm} &= \hat{s} - \tilde{\mu}_{\pm}^2, & \tilde{\mathbf{m}}_{\pm} &= m_{\mathbb{D}} \pm m_{\mathbb{V}}, & \hat{\sigma}_{\pm} &= \mathbf{M}_{\pm}^2 - \hat{s}.
\end{aligned} \tag{B5}$$

In the SM, the FCNC charmed-hadron decays with neutrinos in the final states get short-distance contributions arising from loop diagrams and brought about by the effective Hamiltonian

$$\mathcal{H}_{c \rightarrow u \nu \bar{\nu}}^{\text{SM}} = \frac{\alpha_e G_F}{\sqrt{2} \pi \sin^2 \theta_W} \sum_{\ell=e, \mu, \tau} \sum_{q=d, s, b} \hat{\lambda}_q \bar{D}(r_q, r_\ell) \bar{u} \gamma^\eta P_L c \bar{\nu}_\ell \gamma_\eta P_L \nu_\ell, \tag{B6}$$

where G_F denotes the Fermi constant, θ_W is the Weinberg angle, the factor $\hat{\lambda}_q = V_{uq}^* V_{cq}$ comprises Cabibbo-Kobayashi-Maskawa (CKM) matrix elements, $r_f = m_f^2/m_W^2$, and the loop function [62]

$$\bar{D}(x, y) = \frac{x(4-y)^2}{8(1-y)^2} \frac{y \ln y}{x-y} + \frac{x(4-x)^2}{8(1-x)^2} \frac{x \ln x}{y-x} + \frac{4-2x+x^2}{8(1-x)^2} x \ln x - \frac{4+2x+5y-2xy}{8(1-x)(1-y)} x. \tag{B7}$$

Accordingly, in the notation of eq. (B1), each ℓ term in eq. (B6) yields

$$\mathbf{C}_{\mathbf{f}\mathbf{f}'}^{\mathbb{V}} = -\mathbf{C}_{\mathbf{f}\mathbf{f}'}^{\mathbb{A}} = -\tilde{\mathbf{C}}_{\mathbf{f}\mathbf{f}'}^{\mathbb{V}} = \tilde{\mathbf{C}}_{\mathbf{f}\mathbf{f}'}^{\mathbb{A}} = \sum_{q=d, s, b} \frac{\alpha_e G_F \hat{\lambda}_q \bar{D}(r_q, r_\ell)}{4\sqrt{2} \pi \sin^2 \theta_W}, \tag{B8}$$

with $\mathbf{f} = \mathbf{f}' = \nu_\ell$. Incorporating this into eqs. (B3) and (B4), employing the form factors specified in the previous appendix and the values of the parameters in eq. (B6) and of the relevant hadron lifetimes and particle masses from ref. [27], with $m_{\mathbf{f}} = m_{\mathbf{f}'} = 0$, and adding the rates corresponding to the $\ell = e, \mu, \tau$ flavors of the neutrinos, we then obtain the predictions listed in eq. (1). The nonzero SM contribution to $D^0 \rightarrow \cancel{E}$ is mainly from $\mathcal{B}(D^0 \rightarrow \nu \bar{\nu} \nu \bar{\nu}) \sim 3 \times 10^{-27}$ [18]. The long-distance contributions are difficult to determine reliably, but estimates for a few modes produced results which could be somewhat bigger than their short-distance counterparts [2, 5, 14], but not

by several orders of magnitude. It follows that the SM backgrounds to our charmed-hadron decays of interest can be safely ignored.

-
- [1] C. Q. Geng, C. C. Lih, and W.-M. Zhang, Study of radiative leptonic D meson decays, *Mod. Phys. Lett. A* **15**, 2087 (2000), [arXiv:hep-ph/0012066](#).
 - [2] G. Burdman, E. Golowich, J. L. Hewett, and S. Pakvasa, Rare charm decays in the standard model and beyond, *Phys. Rev. D* **66**, 014009 (2002), [arXiv:hep-ph/0112235](#).
 - [3] C.-H. Chen, C.-Q. Geng, and T.-C. Yuan, Non-standard neutrino interactions in $K^+ \rightarrow \pi^+ \nu \bar{\nu}$ and $D^+ \rightarrow \pi^+ \nu \bar{\nu}$ decays, *Phys. Rev. D* **75**, 077301 (2007), [arXiv:hep-ph/0703196](#).
 - [4] C.-H. Chen, C.-Q. Geng, and T.-C. Yuan, $D - \bar{D}$ mixing and rare D decays in the Littlest Higgs model with non-unitarity matrix, *Phys. Lett. B* **655**, 50 (2007), [arXiv:0704.0601 \[hep-ph\]](#).
 - [5] J. F. Kamenik and C. Smith, Tree-level contributions to the rare decays $B^+ \rightarrow \pi^+ \nu \bar{\nu}$, $B^+ \rightarrow K^+ \nu \bar{\nu}$, and $B^+ \rightarrow K^{*+} \nu \bar{\nu}$ in the Standard Model, *Phys. Lett. B* **680**, 471 (2009), [arXiv:0908.1174 \[hep-ph\]](#).
 - [6] A. Badin and A. A. Petrov, Searching for light Dark Matter in heavy meson decays, *Phys. Rev. D* **82**, 034005 (2010), [arXiv:1005.1277 \[hep-ph\]](#).
 - [7] I. Doršner, S. Fajfer, A. Greljo, J. F. Kamenik, and N. Košnik, Physics of leptoquarks in precision experiments and at particle colliders, *Phys. Rept.* **641**, 1 (2016), [arXiv:1603.04993 \[hep-ph\]](#).
 - [8] G. Li, T. H. Wang, Y. Jiang, J. B. Zhang, and G. L. Wang, Spin-1/2 invisible particles in heavy meson decays, *Phys. Rev. D* **102**, 095019 (2020), [arXiv:2004.10942 \[hep-ph\]](#).
 - [9] S. Fajfer and A. Novosel, Colored scalars mediated rare charm meson decays to invisible fermions, *Phys. Rev. D* **104**, 015014 (2021), [arXiv:2101.10712 \[hep-ph\]](#).
 - [10] G. Faisel, J.-Y. Su, and J. Tandean, Exploring charm decays with missing energy in leptoquark models, *JHEP* **04**, 246, [arXiv:2012.15847 \[hep-ph\]](#).
 - [11] S. de Boer and G. Hiller, Flavor and new physics opportunities with rare charm decays into leptons, *Phys. Rev. D* **93**, 074001 (2016), [arXiv:1510.00311 \[hep-ph\]](#).
 - [12] R. Bause, H. Gisbert, M. Golz, and G. Hiller, Lepton universality and lepton flavor conservation tests with dineutrino modes, *Eur. Phys. J. C* **82**, 164 (2022), [arXiv:2007.05001 \[hep-ph\]](#).
 - [13] R. Bause, H. Gisbert, M. Golz, and G. Hiller, Rare charm $c \rightarrow u \nu \bar{\nu}$ dineutrino null tests for $e^+ e^-$ machines, *Phys. Rev. D* **103**, 015033 (2021), [arXiv:2010.02225 \[hep-ph\]](#).
 - [14] P. Colangelo, F. De Fazio, and F. Loporco, $c \rightarrow u \nu \nu$ transitions of B_c mesons: 331 model facing Standard Model null tests, *Phys. Rev. D* **104**, 115024 (2021), [arXiv:2107.07291 \[hep-ph\]](#).
 - [15] A. K. Alok, N. R. S. Chundawat, and D. Kumar, Impact of $b \rightarrow s \ell \ell$ anomalies on rare charm decays in non-universal Z' models, *Eur. Phys. J. C* **82**, 30 (2022), [arXiv:2110.12451 \[hep-ph\]](#).
 - [16] M. Golz, G. Hiller, and T. Magorsch, Pinning down $|\Delta c| = |\Delta u| = 1$ couplings with rare charm baryon decays, *Eur. Phys. J. C* **82**, 357 (2022), [arXiv:2202.02331 \[hep-ph\]](#).
 - [17] S. Fajfer, J. F. Kamenik, A. Korajac, and N. Košnik, Correlating New Physics Effects in Semileptonic $\Delta C = 1$ and $\Delta S = 1$ Processes, (2023), [arXiv:2305.13851 \[hep-ph\]](#).
 - [18] B. Bhattacharya, C. M. Grant, and A. A. Petrov, Invisible widths of heavy mesons, *Phys. Rev. D* **99**, 093010 (2019), [arXiv:1809.04606 \[hep-ph\]](#).
 - [19] C.-Q. Geng and G. Li, FCNC processes of charmed hadrons with invisible scalar, *Phys. Lett. B* **839**, 137811 (2023), [arXiv:2212.04699 \[hep-ph\]](#).
 - [20] I. Boiarska, K. Bondarenko, A. Boyarsky, V. Gorkavenko, M. Ovchinnikov, and A. Sokolenko, Phenomenology of GeV-scale scalar portal, *JHEP* **11**, 162, [arXiv:1904.10447 \[hep-ph\]](#).

- [21] J. Martin Camalich, M. Pospelov, P. N. H. Vuong, R. Ziegler, and J. Zupan, Quark Flavor Phenomenology of the QCD Axion, *Phys. Rev. D* **102**, 015023 (2020), [arXiv:2002.04623 \[hep-ph\]](#).
- [22] G. Li, T. H. Wang, Y. Jiang, X. Z. Tan, and G. L. Wang, The study of light invisible particles in B_c decays, *JHEP* **03**, 028, [arXiv:1810.03280 \[hep-ph\]](#).
- [23] E. Gabrielli, B. Mele, M. Raidal, and E. Venturini, FCNC decays of standard model fermions into a dark photon, *Phys. Rev. D* **94**, 115013 (2016), [arXiv:1607.05928 \[hep-ph\]](#).
- [24] M. Fabbrichesi, E. Gabrielli, and G. Lanfranchi, The Dark Photon [10.1007/978-3-030-62519-1](#) (2020), [arXiv:2005.01515 \[hep-ph\]](#).
- [25] J.-Y. Su and J. Tandean, Seeking massless dark photons in the decays of charmed hadrons, *Phys. Rev. D* **102**, 115029 (2020), [arXiv:2005.05297 \[hep-ph\]](#).
- [26] W. Altmannshofer and F. Archilli, Rare decays of b and c hadrons, in *Snowmass 2021* (2022) [arXiv:2206.11331 \[hep-ph\]](#).
- [27] R. L. Workman *et al.* (Particle Data Group), Review of Particle Physics, *PTEP* **2022**, 083C01 (2022).
- [28] Y. T. Lai *et al.* (Belle), Search for D^0 decays to invisible final states at Belle, *Phys. Rev. D* **95**, 011102 (2017), [arXiv:1611.09455 \[hep-ex\]](#).
- [29] M. Ablikim *et al.* (BESIII), Search for the decay $D^0 \rightarrow \pi^0 \nu \bar{\nu}$, *Phys. Rev. D* **105**, L071102 (2022), [arXiv:2112.14236 \[hep-ex\]](#).
- [30] M. Ablikim *et al.* (BESIII), Search for a massless dark photon in $\Lambda_c^+ \rightarrow p \gamma'$ decay, *Phys. Rev. D* **106**, 072008 (2022), [arXiv:2208.04496 \[hep-ex\]](#).
- [31] M. Ablikim *et al.* (BESIII), Future Physics Programme of BESIII, *Chin. Phys. C* **44**, 040001 (2020), [arXiv:1912.05983 \[hep-ex\]](#).
- [32] W. Altmannshofer *et al.* (Belle-II), The Belle II Physics Book, *PTEP* **2019**, 123C01 (2019), [arXiv:1808.10567 \[hep-ex\]](#).
- [33] M. Achasov *et al.*, STCF Conceptual Design Report: Volume I - Physics & Detector, (2023), [arXiv:2303.15790 \[hep-ex\]](#).
- [34] M. Dong *et al.* (CEPC Study Group), CEPC Conceptual Design Report: Volume 2 - Physics & Detector, (2018), [arXiv:1811.10545 \[hep-ex\]](#).
- [35] A. Abada *et al.* (FCC), FCC Physics Opportunities: Future Circular Collider Conceptual Design Report Volume 1, *Eur. Phys. J. C* **79**, 474 (2019).
- [36] C. Bird, P. Jackson, R. V. Kowalewski, and M. Pospelov, Search for dark matter in $b \rightarrow s$ transitions with missing energy, *Phys. Rev. Lett.* **93**, 201803 (2004), [arXiv:hep-ph/0401195 \[hep-ph\]](#).
- [37] C. Bird, R. V. Kowalewski, and M. Pospelov, Dark matter pair-production in $b \rightarrow s$ transitions, *Mod. Phys. Lett.* **A21**, 457 (2006), [arXiv:hep-ph/0601090 \[hep-ph\]](#).
- [38] C. S. Kim, S. C. Park, K. Wang, and G. Zhu, Invisible Higgs decay with $B \rightarrow K \nu \bar{\nu}$ constraint, *Phys. Rev.* **D81**, 054004 (2010), [arXiv:0910.4291 \[hep-ph\]](#).
- [39] X.-G. He, S.-Y. Ho, J. Tandean, and H.-C. Tsai, Scalar Dark Matter and Standard Model with Four Generations, *Phys. Rev. D* **82**, 035016 (2010), [arXiv:1004.3464 \[hep-ph\]](#).
- [40] J. F. Kamenik and C. Smith, FCNC portals to the dark sector, *JHEP* **03**, 090, [arXiv:1111.6402 \[hep-ph\]](#).
- [41] J.-Y. Su and J. Tandean, Searching for dark photons in hyperon decays, *Phys. Rev. D* **101**, 035044 (2020), [arXiv:1911.13301 \[hep-ph\]](#).
- [42] Y. Liao, H.-L. Wang, C.-Y. Yao, and J. Zhang, Imprint of a new light particle at KOTO?, *Phys. Rev. D* **102**, 055005 (2020), [arXiv:2005.00753 \[hep-ph\]](#).
- [43] X.-G. He, X.-D. Ma, J. Tandean, and G. Valencia, Evading the Grossman-Nir bound with $\Delta I = 3/2$ new physics, *JHEP* **08** (08), 034, [arXiv:2005.02942 \[hep-ph\]](#).
- [44] S. Gori, G. Perez, and K. Tobioka, KOTO vs. NA62 Dark Scalar Searches, *JHEP* **08**, 110,

arXiv:2005.05170 [hep-ph].

- [45] J.-Y. Su and J. Tandean, Kaon decays shedding light on massless dark photons, *Eur. Phys. J. C* **80**, 824 (2020), arXiv:2006.05985 [hep-ph].
- [46] G. Li, T. H. Wang, J. B. Zhang, and G. L. Wang, The light invisible boson in FCNC decays of B and B_c mesons, *Eur. Phys. J. C* **81**, 564 (2021), arXiv:2103.12921 [hep-ph].
- [47] X.-G. He, X.-D. Ma, and G. Valencia, FCNC B and K meson decays with light bosonic Dark Matter, *JHEP* **03**, 037, arXiv:2209.05223 [hep-ph].
- [48] W. Altmannshofer, B. V. Lehmann, and S. Profumo, Cosmological implications of the KOTO excess, *Phys. Rev. D* **102**, 083527 (2020), arXiv:2006.05064 [hep-ph].
- [49] C.-Q. Geng and J. Tandean, Probing new physics with the kaon decays $K \rightarrow \pi\pi \cancel{E}$, *Phys. Rev. D* **102**, 115021 (2020), arXiv:2009.00608 [hep-ph].
- [50] M. Hostert and M. Pospelov, Novel multilepton signatures of dark sectors in light meson decays, *Phys. Rev. D* **105**, 015017 (2022), arXiv:2012.02142 [hep-ph].
- [51] G. Li, J.-Y. Su, and J. Tandean, Flavor-changing hyperon decays with light invisible bosons, *Phys. Rev. D* **100**, 075003 (2019), arXiv:1905.08759 [hep-ph].
- [52] B. Dutta, S. Ghosh, and T. Li, Explaining $(g-2)_{\mu,e}$, the KOTO anomaly and the MiniBooNE excess in an extended Higgs model with sterile neutrinos, *Phys. Rev. D* **102**, 055017 (2020), arXiv:2006.01319 [hep-ph].
- [53] J.-Y. Su and J. Tandean, Exploring leptoquark effects in hyperon and kaon decays with missing energy, *Phys. Rev. D* **102**, 075032 (2020), arXiv:1912.13507 [hep-ph].
- [54] X. G. He and G. Valencia, $R_{K^{(*)}}^\nu$ and non-standard neutrino interactions, *Phys. Lett. B* **821**, 136607 (2021), arXiv:2108.05033 [hep-ph].
- [55] G. Li, C.-W. Liu, and C.-Q. Geng, Bottomed baryon decays with invisible Majorana fermions, *Phys. Rev. D* **106**, 115007 (2022), arXiv:2206.01575 [hep-ph].
- [56] A. M. Sirunyan *et al.* (CMS), Searches for physics beyond the standard model with the M_{T2} variable in hadronic final states with and without disappearing tracks in proton-proton collisions at $\sqrt{s} = 13$ TeV, *Eur. Phys. J. C* **80**, 3 (2020), arXiv:1909.03460 [hep-ex].
- [57] D. E. Hazard and A. A. Petrov, Radiative lepton flavor violating B , D , and K decays, *Phys. Rev. D* **98**, 015027 (2018), arXiv:1711.05314 [hep-ph].
- [58] A. Bazavov *et al.* (Fermilab Lattice, MILC), D-meson semileptonic decays to pseudoscalars from four-flavor lattice QCD, (2022), arXiv:2212.12648 [hep-lat].
- [59] H.-Y. Xing, Z.-N. Xu, Z.-F. Cui, C. D. Roberts, and C. Xu, Heavy + heavy and heavy + light pseudoscalar to vector semileptonic transitions, *Eur. Phys. J. C* **82**, 889 (2022), arXiv:2205.13642 [hep-ph].
- [60] S. Meinel, $\Lambda_c \rightarrow N$ form factors from lattice QCD and phenomenology of $\Lambda_c \rightarrow n\ell^+\nu_\ell$ and $\Lambda_c \rightarrow p\mu^+\mu^-$ decays, *Phys. Rev. D* **97**, 034511 (2018), arXiv:1712.05783 [hep-lat].
- [61] C. Q. Geng, C.-W. Liu, and T.-H. Tsai, Semileptonic weak decays of antitriplet charmed baryons in the light-front formalism, *Phys. Rev. D* **103**, 054018 (2021), arXiv:2012.04147 [hep-ph].
- [62] T. Inami and C. S. Lim, Effects of Superheavy Quarks and Leptons in Low-Energy Weak Processes $K_L \rightarrow \mu\bar{\mu}$, $K^+ \rightarrow \pi^+\nu\bar{\nu}$, and $K^0 \leftrightarrow \bar{K}^0$, *Prog. Theor. Phys.* **65**, 297 (1981).